



Research paper

Manipulation of gut microbiota blunts the ventilatory response to hypercapnia in adult rats



Karen M. O'Connor^{a,b,c}, Eric F. Lucking^a, Anna V. Golubeva^c, Conall R. Strain^d, Fiona Fouhy^{c,d}, María C. Cenit^{b,e}, Pardeep Dhaliwal^a, Thomaz F.S. Bastiaanssen^{b,c}, David P. Burns^a, Catherine Stanton^{c,d}, Gerard Clarke^{c,f}, John F. Cryan^{b,c}, Ken D. O'Halloran^{a,c,*}

^a Department of Physiology, School of Medicine, College of Medicine & Health, University College Cork, Cork, Ireland

^b Department of Anatomy & Neuroscience, School of Medicine, College of Medicine & Health, University College Cork, Cork, Ireland

^c APC Microbiome Ireland, University College Cork, Cork, Ireland

^d Teagasc Food Research Centre, Moorepark, Fermoy, County Cork, Ireland

^e Institute of Agrochemistry and Food Technology (IATA), National Council for Scientific Research (CSIC), Valencia, Spain

^f Department of Psychiatry and Neurobehavioural Science, School of Medicine, College of Medicine & Health, University College Cork, Cork, Ireland

ARTICLE INFO

Article history:

Received 10 December 2018

Received in revised form 8 March 2019

Accepted 11 March 2019

Available online 18 March 2019

Keywords:

Antibiotics
 Faecal microbiota transfer
 Breathing
 Hypercapnia
 Cardiovascular
 Vagus
 Neurochemistry
 Intestinal permeability
 Microbiota

ABSTRACT

Background: It is increasingly evident that perturbations to the diversity and composition of the gut microbiota have significant consequences for the regulation of integrative physiological systems. There is growing interest in the potential contribution of microbiota–gut–brain signalling to cardiorespiratory control in health and disease. **Methods:** In adult male rats, we sought to determine the cardiorespiratory effects of manipulation of the gut microbiota following a 4-week administration of a cocktail of antibiotics. We subsequently explored the effects of administration of faecal microbiota from pooled control (vehicle) rat faeces, given by gavage to vehicle- and antibiotic-treated rats.

Findings: Antibiotic intervention depressed the ventilatory response to hypercapnic stress in conscious animals, owing to a reduction in the respiratory frequency response to carbon dioxide. Baseline frequency, respiratory timing variability, and the expression of apnoeas and sighs were normal. Microbiota-depleted rats had decreased systolic blood pressure. Faecal microbiota transfer to vehicle- and antibiotic-treated animals also disrupted the gut microbiota composition, associated with depressed ventilatory responsiveness to hypercapnia. Chronic antibiotic intervention or faecal microbiota transfer both caused significant disruptions to brainstem monoamine neurochemistry, with increased homovanillic acid:dopamine ratio indicative of increased dopamine turnover, which correlated with the abundance of several bacteria of six different phyla.

Interpretation: Chronic antibiotic administration and faecal microbiota transfer disrupt gut microbiota, brainstem monoamine concentrations and the ventilatory response to hypercapnia. We suggest that aberrant microbiota–gut–brain axis signalling has a modulatory influence on respiratory behaviour during hypercapnic stress.

Funding: Department of Physiology and APC Microbiome Ireland, University College Cork, Ireland.

© 2019 Published by Elsevier B.V. This is an open access article under the CC BY-NC-ND license (<http://creativecommons.org/licenses/by-nc-nd/4.0/>).

Abbreviations: ABX, antibiotic-treated; AIH, acute intermittent hypoxia; BH, Benjamini–Hochberg; DA, dopamine; Dia, diaphragm; EMG, electromyogram; ETCO₂, end-tidal carbon dioxide; FDR, false discovery rate; FLASH, fast length adjustment of short reads to improve genome assemblies; FMT, faecal microbiota transfer; *f_R*, respiratory frequency; FiCO₂, fractional inspired carbon dioxide concentration; FiO₂, fractional inspired oxygen concentration; Hb, haemoglobin; HVA, homovanillic acid; L-DOPA, L-3,4-dihydroxyphenylalanine; NA, noradrenaline; OTUs, operational taxonomic units; PBG, phenylbiguanide; PBS, phosphate buffered saline; PCoA, Principal coordinates analysis; PaCO₂, partial pressure of arterial carbon dioxide; PD whole tree, phylogenetic whole tree diversity; PaO₂, partial pressure of arterial oxygen; QIIME, quantitative insights into microbial ecology; SaO₂, arterial oxygen saturation; SD1, short-term respiratory timing variability; SD2, long-term respiratory timing variability; T_e, expiratory time; T_i, inspiratory time; T_{tot}, total breath duration; VCO₂, carbon dioxide; V_E, minute ventilation production; VEH, vehicle autoclaved deionised water; V_E/VCO₂, ventilatory equivalent for CO₂; VO₂, oxygen consumption; V_T, tidal volume; V_T/T_i, mean inspiratory flow; 5-HIAA, 5-hydroxyindoleacetic acid; 5-HT, 5-hydroxytryptamine (serotonin); 5-HT₃, 5-hydroxytryptamine type 3.

* Corresponding author at: Department of Physiology, University College Cork, Western Gateway Building, Western Road, Cork, Ireland.

E-mail address: k.ohalloran@ucc.ie (K.D. O'Halloran).

Research in context

Evidence before this study

The microbiota-gut-brain axis is implicated in the homeostatic control of physiological systems; however, its potential influence on the control of breathing is unclear.

Added value of this study

Chronic antibiotic administration in rats depleted gut microbiota, increased gut permeability, altered brainstem neurochemistry and depressed the ventilatory response to hypercapnic stress. Faecal microbiota transfer in vehicle- and antibiotic-treated rats significantly disrupted the microbiota composition, with associated disruptions to brainstem neurochemistry and depressed ventilation during hypercapnia. Brainstem monoamine neurochemistry correlated with the relative abundance of several bacteria, primarily of the Firmicutes phylum.

Implications of all the available evidence

Manipulation of the gut microbiota disrupts respiratory behaviour suggesting that the microbiota-gut-brain axis has the capacity to alter respiratory control through aberrant neuromodulation of breathing.

1. Introduction

There is a growing understanding of the significance of the gastrointestinal microbiome and its modulatory capacity in the homeostatic regulation of multiple physiological systems [1]. Trillions of gut microbiota form a co-dependent, mutualistic relationship with the host, contributing to whole-body health [2], through an extensive multimodal communication pathway termed the 'microbiota-gut-brain axis' [3]. Dysregulated microbiota-gut-brain axis signalling disrupts major neurocontrol systems affecting anxiety, pain, depression and social behaviours [4–10]. Multiple contributors to microbiota-gut-brain axis communication have been identified, including neural pathways, immune mediators, bacterial metabolites, serotonin and tryptophan metabolism, host genetics and gut hormones [11]. There is a wide appreciation of the potential contribution of microbiota-gut-brain signalling to cardiorespiratory control in health and disease [12–17].

The cardiorespiratory system is tightly regulated by neuronal networks residing within the brainstem. Respiratory rhythm and pattern, generated by complex brainstem networks is transduced *via* multiple efferent pathways, directly or indirectly *via* the spinal nuclei to the striated muscles of breathing, which provides for exquisite breath-by-breath control of pulmonary ventilation [18,19]. Autonomic centres within the medulla oblongata (dorsal motor nucleus of the vagus, nucleus ambiguus and rostral ventrolateral medulla) transduce parasympathetic and sympathetic motor outflow to the heart and circulation. Of interest, there is considerable respiratory-related modulation of autonomic efferent signalling. The vagus nerve, a key bi-directional communication pathway of the microbiota-gut-brain axis [20], provides visceral information from sensors in multiple peripheral sites to the nucleus of the solitary tract within the brainstem. There is considerable sensory-cued modulation of respiratory motor and autonomic outputs, from the periphery, which execute efficient cardiorespiratory control. Notwithstanding the primary homeostatic function of the neural networks governing breathing and blood pressure regulation, there is ample evidence in support of a remarkable capacity for plasticity at

multiple sites within the control network, both at a central and peripheral level, which underpin adaptive and maladaptive outcomes [21–25].

Maladaptive plasticity expressed in several stress models have revealed considerable long-lasting perturbations to respiratory control, with deleterious consequences for whole-body health [26–30]. Prenatal stress results in enhanced respiratory variability and alters ventilatory control during hypoxic and hypercapnic chemostimulation in rat offspring during adulthood [15]. Interestingly, respiratory frequency responses to hypercapnia correlated with alterations in the gut microbiota [15]. Recently, exposure to chronic intermittent hypoxia, modelling human sleep apnoea, was shown to disrupt cardiorespiratory homeostasis, with evidence of decreased prevalence of protective sigh behaviours, altered autonomic control of heart rate, decreased brainstem noradrenaline concentration, and altered gut microbiota composition [16]. To our knowledge, there are no other studies of the effects of manipulation of the microbiota on the control of breathing. Yet importantly, animal models of sleep-disordered breathing show evidence of altered microbiota composition and diversity, driven by altered diet and/or exposure to intermittent hypoxia [12,31–33]. Thus, it appears that respiratory dysregulation has the capacity to alter the microbiota. It is important to determine if disruption to the microbiota affects respiratory homeostasis.

Of relevance, the gut microbiota are important modulators of cardiovascular control. The transfer of faeces from hypertensive donors (spontaneously hypertensive rats, a hypertensive model of sleep-disordered breathing fed a high-fat diet, and hypertensive human donors) into normotensive recipient or germ-free animals leads to the development of hypertension in the recipient animal [12,14,34,35]. A decrease in butyrate-producing and an increase in lactate-producing bacteria are associated with a hypertensive phenotype [12,14,35]. More recently, it was established in an animal model of obstructive sleep apnoea that acetate is a key player in blood pressure regulation [17]. Collectively, these findings suggest an influential role for the microbiota-gut brain axis in cardiovascular homeostasis.

It is established that chronic administration of a cocktail of broad-spectrum antibiotics significantly depletes the gut microbiota [36,37]. It is also recognised that alterations to the gut microbiota can influence brain behaviours at a functional level [5,6,8,36]. Thus, we sought to perform a comprehensive assessment of cardiorespiratory physiology in the context of a manipulated gut microbiota. We examined cardiorespiratory control and reflex responsiveness in adult rats following a 4-week antibiotic intervention period. We hypothesised that there would be evidence of aberrant plasticity in cardiorespiratory control in antibiotic-treated rats. Thereafter, in a subset of animals, we explored if manipulation of the microbiota *via* faecal microbiota transfer could reverse or ameliorate the putative deleterious effects of antibiotic intervention on cardiorespiratory control.

2. Methods

2.1. Ethical approval

All procedures on live animals were performed under licence from the Government of Ireland Department of Health (B100/4498) in accordance with National and European Union directive 2010/63/EU, with prior ethical approval by University College Cork (AEEC #2013/035). Experiments were conducted in accordance with guidelines established by University College Cork's Animal Welfare Body.

2.2. Experiment animals

Ten-week old adult male Sprague Dawley rats ($n = 40$; purchased from Envigo, UK) were housed as age-matched pairs in standard rat cages. All animals were housed under a 12-h light: 12-h dark cycle with standard rodent chow available *ad libitum*.

2.3. Antibiotic administration

Rats were randomly allocated to receive autoclaved deionised water (vehicle, VEH; $n = 20$) or broad-spectrum antibiotics (ABX; $n = 20$) in autoclaved deionised water for 4-weeks. To deplete the microbiota, we used an antibiotic cocktail consisting of ampicillin (1 g/l), vancomycin (500 mg/l), ciprofloxacin (20 mg/l), imipenem (250 mg/l) and metronidazole (1 g/l) [5,36]. Water bottles were replenished every second day and water consumption recorded per cage. Animal body weights were monitored daily (Supplementary Fig. 1a). Weight loss in the beginning of ABX intervention is a commonly reported side effect related to the aversive taste of the ABX cocktail. Fresh bedding was given to ABX and VEH groups every other day to decrease the risk of microbiota re-establishment in ABX animals.

2.4. Faecal microbiota transfer (FMT) protocol

2.4.1. Collection and processing of donor microbiota for faecal microbiota transplantation

Donor faecal microbiota was acquired from the pooled faeces of 10 VEH rats, collected fresh from individual animals by massaging the lower abdomen and promoting the passage of faeces from the rats. Both the collection and the transportation and processing of faeces occurred under anaerobic conditions to prevent loss of anaerobic microbiota. Sterile reduced phosphate-buffered saline (PBS; 10 ml) containing 20% glycerol (v/v) was added to each 1 g of pooled faeces. The faecal material was thoroughly re-suspended. Samples were centrifuged at 2000 rpm for 5 min at 4 °C (MIKRO 22R refrigerated centrifuge) to generate a sediment of undigested dietary fibres. Supernatants were aliquoted, frozen and stored at -80 °C until use in oral gavage.

2.4.2. Administration of FMT

ABX rats ($n = 10$) received a washout period of autoclaved deionised water for three days and VEH rats ($n = 10$) remained on autoclaved deionised water. Two inoculations of donor microbiota (300 μ l) were administered *via* oral gavage to ABX and VEH rats, on day 1 and day 7 following the washout period. To reinforce the donor microbiota phenotype, the ABX rats were transferred to bedding previously occupied by VEH rats on inoculation day 1 and thereafter on a weekly basis (ABX-FMT group). VEH rats were transferred to fresh

bedding adhering to the pattern described above (VEH-FMT group). All animals received autoclaved deionised water for the duration of the 4-week period (Fig. 1).

2.5. Assessment of respiratory flow and metabolism in unrestrained, unanaesthetised rats

2.5.1. Whole-body plethysmography

Whole-body plethysmography (DSI, St. Paul, Minnesota, USA) was used to record respiratory flow during quiet rest in unrestrained, unanaesthetised rats. This was performed at the animal housing facility of University College Cork as this subset of animals subsequently remained in the facility for faecal microbiota transfer and housing for a further period of 4 weeks (Section 2.4.2). Animals were introduced into custom chambers (601-1427-001 PN, DSI) with room air pumped through the chambers (3 l/min) ensuring the maintenance of oxygen (O_2) and carbon dioxide (CO_2). Animals were allowed to acclimate for 30–90 min to allow habituation to the surroundings. Contemporaneous observations were performed in ABX ($n = 10$) versus VEH ($n = 10$) and subsequently ABX-FMT ($n = 10$) versus VEH-FMT ($n = 10$) using a pair of plethysmograph chambers.

2.5.2. Metabolic measurements

CO_2 production (VCO_2) and O_2 consumption (VO_2) were measured in animals throughout the whole-body plethysmography protocol (O_2 and CO_2 analyser; AD Instruments, Colorado Springs, CO, USA) as previously described [38–41].

2.5.3. Experimental protocol

Once the acclimation period was complete, a 10–15-min steady-state normoxia period allowed for the assessment of baseline parameters ($FiO_2 = 0.21$; balance N_2). Thereafter, rats were exposed to a 10-min poikilocapnic hypoxia challenge ($FiO_2 = 0.10$; balance N_2). Each animal was then allowed to recover during normoxia ($FiO_2 = 0.21$; balance N_2) to re-establish stable breathing. Subsequently, another baseline period was recorded and rats were then exposed to a hypercapnic challenge ($FiCO_2 = 0.05$; balance O_2) for 10 min followed by a recovery period. A new baseline period was determined and animals were then exposed to 10 successive cycles of acute intermittent hypoxia (AIH), consisting of alternating periods of normoxia ($FiO_2 = 0.21$; balance

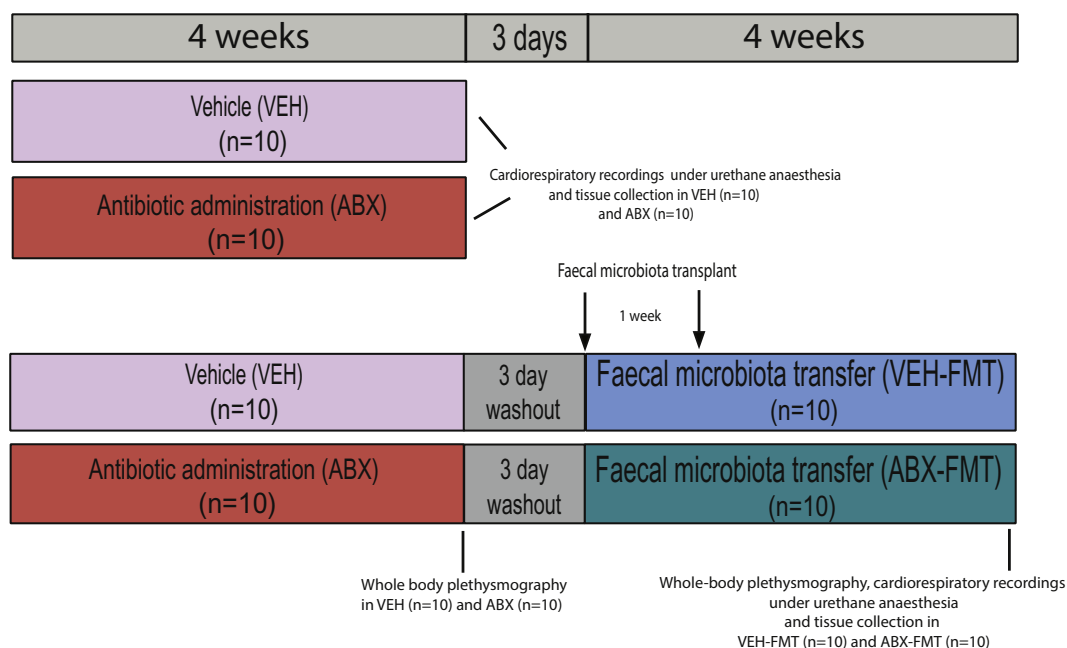


Fig. 1. Experimental design. Schematic representation of the experimental design employed in the study.

N₂) for 6 min and hypoxia (FiO₂ = 0.10, balance N₂) for 6 min. Following the AIH protocol, a normoxia period was established (FiO₂ = 0.21; balance N₂) for 1 h. On completion of the experimental protocol, faecal pellets in the plethysmograph chambers were counted per unit time.

2.5.4. Data analysis for whole-body plethysmography and metabolism

Respiratory parameters including respiratory frequency (f_R), tidal volume (V_T), minute ventilation (V_E), inspiratory time (T_i) and expiratory time (T_e) were recorded on a breath-by-breath basis for analysis (Finepoint software Buxco Research Systems, Wilmington, NC, USA). Artefacts in the signals due to movement and sniffing were excluded from analysis. A steady-state baseline period was averaged during normoxia to assess ventilatory and metabolic parameters at quiet rest. For acute hypoxic and hypercapnic challenges, respiratory and metabolic data were averaged for the last 5 min of these exposures to ensure adequate time for gas mixing in the chambers and assessment of steady-state ventilatory and metabolic responses. Data are expressed as a change in the absolute values from baseline values. Furthermore, to determine the peak hypoxic ventilatory response, respiratory frequency was averaged every 10 s for the first 120 s of the acute hypoxic gas challenge. Similarly, for the acute hypercapnic challenge, the respiratory frequency response was averaged for each minute of the 10-min challenge. For AIH challenges, respiratory data were compared between groups for the last hypoxia challenge and expressed as a percentage change from the preceding baseline normoxia exposure. Data from the post-AIH normoxic period was collected at 5 min intervals. The last 5-min epoch of the 1-h period of normoxia following exposure to AIH was compared with the normoxic baseline period preceding AIH and expressed as percentage change from baseline as a measure of AIH-induced respiratory plasticity. Comparisons were made between the experimental groups. Respiratory flow signals were also analysed to quantify the occurrence of apnoeas (post-sigh apnoeas and spontaneous apnoeas) and augmented breaths (sighs) during normoxic baseline and hypoxic and hypercapnic breathing as previously described [42]. An apnoea was defined as two consecutive missed breaths and data are expressed as apnoea index (number of apnoeas per hour). Sighs (augmented breaths) were distinguished as breaths with double the amplitude of the average V_T . Poincaré plots were constructed showing breath-to-breath (BBn) versus the subsequent breath-to-breath interval (BBn + 1) allowing determination of short-term (SD1) and long-term (SD2) respiratory timing variability during stable baseline as well as hypoxia and hypercapnia breathing. V_T , V_E , V_T/T_i , VO_2 and VCO_2 were normalised per 100 g body mass.

2.6. Assessment of cardiorespiratory parameters under urethane anaesthesia

2.6.1. Surgical protocol and cardiorespiratory measures

Cardiorespiratory parameters were assessed in rats under urethane anaesthesia (1.5 g/kg i.p.; 20% w/v) following isoflurane induction (5% by inhalation in room air). Depth of anaesthesia was assessed throughout the surgical and experimental protocol by carefully monitoring reflex responses to tail/paw pinch and the corneal reflex. If required, supplemental doses of anaesthetic were given. Rats were placed in the supine position and core body temperature was maintained at 37 °C using a homeothermic blanket system (Harvard Apparatus, Holliston, MA, USA) and a rectal temperature probe.

A mid-cervical tracheotomy was performed. The right jugular vein was then cannulated for intravenous (i.v.) infusion of supplemental anaesthetic and drugs. Next, the right carotid artery was cannulated and a pressure catheter inserted into the left ventricle to record left ventricular contractility (dP/dt max); artefacts were observed in the pressure signals in some animals and data acquired from these animals was excluded. The femoral artery was cannulated for the recording of arterial blood pressure and the withdrawal of arterial blood samples for blood gas, pH and electrolyte analysis (i-STAT; Abbott Laboratories Ltd). All

rats were maintained with a bias flow of supplemental O₂ to preserve arterial oxygen saturation above 95% during basal conditions (SaO₂; Starr Life Sciences, PA, USA). A pneumotachometer and a CO₂ analyser (microCapStar End-Tidal CO₂ analyser; CWE Inc., USA) were connected to a tracheal cannula to determine tracheal flow and end-tidal CO₂ (ETCO₂), respectively. A concentric needle electrode (26G; Natus Manufacturing Ltd., Ireland) was inserted into the costal diaphragm for the continuous measurement of diaphragm electromyogram (EMG) activity. Signals were amplified (x5,000), filtered (band pass; 500–5000 Hz) and integrated (50 ms time constant; Neurolog system, Digitimer Ltd., UK). LabChart v7 (ADInstruments) was used to display data in real-time.

2.6.2. Experimental protocol

An arterial blood gas sample was attained following a 30-minute period of stabilisation. Following the stabilisation period, baseline parameters were assessed for 10 min. An electronic gas mixer (GSM-3 Gas Mixer; CWE Inc.) was used to manipulate the gas composition of the bias flow to administer chemostimulation challenges to the rat. The rats were exposed to a graded hypercapnic challenge: FiCO₂ = 0.05 and 0.10 (supplemental O₂; balance N₂) consecutively for 5 min each. Following a recovery period, animals were challenged with poikilocapnic hypoxia (FiO₂ = 0.10, balance N₂) for 5 min, followed by a 5 min hypoxic hypercapnic challenge (FiO₂ = 0.10, FiCO₂ = 0.05, balance N₂). After the chemostimulation challenges and a sufficient recovery period, the serotonin type 3 (5-HT₃) receptor agonist phenylbiguanide was administered in incremental doses (PBG; 2, 4, 8, 16, 32 µg/kg; i.v.) to stimulate pulmonary vagal afferent C-fibres [43,44]. Then animals underwent bilateral cervical vagotomy. After a 20-min recovery period, another blood gas sample was acquired and post-vagotomy baseline parameters were determined. The chemostimulation challenges described above were repeated under vagotomised conditions. Finally, a single bolus of 32 µg/kg PBG was administered to confirm that PBG-induced pulmonary chemoreflex responses were entirely dependent upon vagal nerve transmission.

Animals were euthanised by urethane overdose i.v. and whole brains were immediately harvested and frozen in –80 °C isopentane and stored at –80 °C until required. The caecum was removed, weighed and caecal contents were removed rapidly and snap frozen in liquid nitrogen. The distal ileum and proximal colon were removed. The heart was removed and the right ventricle and left ventricle + septum were separated and weighed. The lungs were removed and weighed and then were allowed to air dry at 37 °C for at least 48 h and re-weighed.

2.6.3. Data analysis of cardiorespiratory parameters in anaesthetised rats

10 min of stable recording were averaged (baseline data) and are presented as absolute values. For cardiorespiratory and EMG responses during graded hypercapnia, hypoxia, hypoxic hypercapnia, vagotomy and chemostimulation challenges post-vagotomy, for each reported parameter, the average of the last minute of recordings was determined and data were compared with the 1-minute pre-challenge baseline. To assess the dynamic response to PBG administration, data were averaged in 3-second bins and the maximal response for each concentration was determined for each cardiorespiratory parameter reported. Cardiovascular responses to PBG were expressed as absolute change from the preceding baseline value. Maximum apnoea and post-apnoea tachypnoea data from PBG stimulation were expressed as the duration of the apnoea or tachypnoea period normalised to the average cycle duration determined during the baseline period preceding PBG challenges i.e. fold change. Cardiorespiratory responses to vagotomy and chemostimulation before and after vagotomy were expressed as absolute change from the preceding baseline. EMG responses to vagotomy and chemostimulation before and after vagotomy were expressed as percent change from the preceding baseline value.

2.7. Macromolecular permeability in small and large intestine *ex vivo*

2.7.1. Epithelial permeability: Ussing chambers

In a subset of animals, distal ileum and proximal colon were removed and examined *ex vivo*. Distal ileum (a 2.0 cm segment adjacent to the caecum) and proximal colon (2.0 cm most distal segment of proximal colon) were gently flushed, cut open along the mesenteric line and mounted in Ussing chambers with an exposed tissue area of 0.12 cm². Tissue was bathed with Krebs solution (in mM: 1.2 NaH₂PO₄; 117 NaCl; 4.8 KCl; 1.2 MgCl₂; 25 NaHCO₃; 11 CaCl₂ and 10 glucose) at 37 °C with continuous carbogen (95% O₂, 5% CO₂) supply. 4-kDa FITC-dextran (4 kDa, FD4, Sigma, Ireland) was added to the mucosal (luminal) chamber at a final concentration of 2.5 mg/ml. To assess FITC flux through the epithelial barrier, samples (200 µl) were collected from the serosal chamber at 0 (baseline), 60 and 120 min after the addition of FITC. At each time-point, the volume removed was replenished with Krebs buffer. To exclude the potential contribution of ileac Na⁺-glucose co-transporter (Slc5a1) to paracellular permeability, glucose in the mucosal chamber buffer was substituted with 10 mM mannitol in ileac tissue samples [45].

2.7.2. Data analysis

FITC was measured on VICTOR-1 plate reader (PerkinElmer) at 485 nm excitation/535 nm emission wavelengths. FITC mucosal-to-serosal flux was calculated as an increment in fluorescence intensity *versus* baseline fluorescence over time and presented as ng/ml.

2.8. Brainstem monoamine concentrations

2.8.1. High-performance liquid chromatography (HPLC) coupled to electrochemical detection for the measurement of brainstem monoamine concentrations

After euthanasia, whole brains were immediately removed from the rats and snap frozen in isopentane cooled in liquid nitrogen. Whole brains were transferred to –80 °C for long-term storage. The frozen brainstem was dissected from the brain at –20 °C and subsequently sonicated in 1 ml of chilled mobile phase spiked with 2 ng/20 µl of *N*-methyl 5-HT (internal standard) (Bandelin Sonolus HD 2070). High-performance liquid chromatography was performed as previously described [16]. The monoamines noradrenaline (NA), dopamine (DA), serotonin (5-HT), monoamine precursor *L*-3,4-dihydroxyphenylalanine (*L*-DOPA) and metabolites 5-hydroxyindoleacetic acid (5-HIAA) and homovanillic acid (HVA) were assessed. Each monoamine and metabolite were identified by their respective characteristic retention times. This was determined by standard injections, which were run at regular intervals during the sample analysis.

2.8.2. Data analysis

Class-VP5 software processed chromatographs that identified specific monoamines. Analyte:internal standard peak response ratios were used to calculate concentrations. Data are expressed as nanograms of neurotransmitter per gram of tissue weight (ng/g).

2.9. 16S rRNA sequence-based microbiota composition and diversity analysis in caecal content

2.9.1. Caecal microbiota DNA extraction and 16S rRNA gene sequencing

DNA extraction and 16S rRNA gene sequencing was performed as previously described [16].

2.9.2. Bioinformatic sequence analysis

FLASH (fast length adjustment of short reads to improve genome assemblies) was used to assemble 300 base paired-end reads. Thereafter, QIIME suite of tools (Quantitative Insights Into Microbial Ecology) version 1.9.0 was used to further process paired-end reads. This processing included quality filtering based on a quality score > 25 and removal of

mismatched barcodes and sequences below length thresholds. Denoising, chimera detection and operational taxonomic units (OTUs) clustering were performed using USEARCH v7 (64-bit) [46]. PyNAST (a flexible tool for aligning sequence to a template alignment) was used to align OTUs. BLAST against the SILVA SSURef database release 123 was used to assign taxonomy. Alpha diversity was generated in QIIME [47].

2.10. Statistical analysis

For data sets with confirmed normal distribution, a one-way ANOVA with Bonferroni *post hoc* where appropriate or parametric two-tailed Student's unpaired *t*-tests with Welch's correction where appropriate were used to test for statistically significant between-group differences. When the assumption of normal distribution was violated, a non-parametric Kruskal-Wallis with Dunn's *post hoc* where appropriate or non-parametric Mann-Whitney *U* tests where appropriate were used. Two-way ANOVA or repeated measures two-way ANOVA with Bonferroni *post hoc* where appropriate were used for relevant data sets. Microbiota data are expressed as median (IQR). All other data sets are expressed as means ± SD or are displayed graphically as box and whisker plots (median, IQR and minimum to maximum values). Microbiota analysis was performed in SPSS and R software environment. The OTUs detected only in ≤ two animals in each group were excluded from the analysis. Bacterial genera that were significantly different at least in one comparison were used to construct the Log₂ fold change ratio heatmap. The 2D principal coordinates analysis (PCoA) plot based on Bray-Curtis distance matrices was constructed using R (version 3.4.4), R Studio (version 1.1.453), and the “vegan” package (version 2.5.1) using the *vegdist* function and recommended parameters. For the correlation analysis between the microbiota composition and a large array of parameters including cardiorespiratory, neuromodulators and intestinal permeability, Hierarchical All-against-All association-testing (HALLA) was used (version 0.8.7) with Spearman correlation as correlation metric and medoid as clustering method. Spearman correlation coefficients were determined for a subset of associations and data are graphically illustrated showing individual data points. GraphPad Prism Software v6 (GraphPad Software, San Diego, CA, USA) was used for all other statistical analysis. Statistical significance was set at *p* < .05. Benjamini-Hochberg (BH) adjustment procedure was applied with the false discovery rate (FDR) set at 10% and 20% to correct for multiple testing in the relative abundance and correlation analyses, respectively. Adobe Illustrator CS5 (v15) was used to edit figs.

3. Results

3.1. Body and tissue weights

Compared with VEH controls, ABX rats tended to be underweight (Supplementary Fig. 1a), coincident with significantly reduced fluid intake during the first week of the experimental protocol (*p* = .001, two-way ANOVA with Bonferroni *post hoc*, Supplementary Fig. 1b). During respiratory assessment in the plethysmograph chambers, manipulation of the gut microbiota altered faecal output per hour (*p* = .04, Kruskal-Wallis, Supplementary Fig. 1c). Microbiota manipulation also significantly altered tissue weights (Table 1).

3.2. Baseline ventilation and metabolism in behaving rats during quiet rest

During baseline breathing, $V_{T,R}$, f_R , and V_E and VCO_2 were all equivalent between groups (Table 2). However, manipulation of the gut microbiota had a significant effect on the ventilatory equivalent for carbon dioxide (V_E/VCO_2) (*p* = .042, one-way ANOVA, Table 2). V_E/VCO_2 was significantly reduced in VEH-FMT rats compared with VEH rats (one-way ANOVA with Bonferroni *post hoc*, Table 2).

Table 1
Body and organ weights.

	VEH (n = 10)	ABX (n = 9)	VEH-FMT (n = 10)	ABX-FMT (n = 10)	One-way ANOVA	VEH vs ABX	VEH-FMT vs ABX-FMT	VEH vs VEH-FMT	ABX vs ABX-FMT	VEH vs ABX-FMT	ABX vs VEH-FMT
Body mass(g)	380 ± 23	369 ± 22	436 ± 27	420 ± 24	<0.0001	0.999	0.888	0.0001	0.0002	0.004	0.0001
RV (mg/100 g)	58 ± 6	51 ± 3	55 ± 7	61 ± 6	0.009	0.133	0.196	0.999	0.008	0.999	0.999
LV (mg/100 g)	219 ± 14	207 ± 10	206 ± 14	208 ± 9	0.053	–	–	–	–	–	–
LV + RV (mg/100 g)	277 ± 16	258 ± 10	260 ± 14	269 ± 11	0.011	0.018	0.982	0.043	0.483	0.967	0.999
Lung dry weight (mg/100 g)	100 ± 12	90 ± 11	98 ± 9	85 ± 10	0.01	0.217	0.067	0.999	0.999	0.015	0.723
Lung wet weight (mg/100 g)	495 ± 104	404 ± 44	427 ± 43	406 ± 83	0.03	0.064	0.999	0.288	0.999	0.061	0.999
Oedema index (% wet weight)	79 ± 3	78 ± 1	77 ± 1	79 ± 3	0.017	0.999	0.196	0.112	0.999	0.999	0.016

BW, body weight; RV, right ventricle; LV, left ventricle; VEH, autoclaved deionised water; ABX, antibiotic-treated; VEH-FMT, VEH followed by faecal microbiota transfer; ABX-FMT, antibiotic-treated followed by faecal microbiota transfer. Data are shown as mean ± SD and were statistically compared using one-way ANOVA with Bonferroni *post hoc* where appropriate, or non-parametric Kruskal-Wallis test with Dunn's *post hoc*, where appropriate. Each *p*-value is adjusted to account for multiple comparisons. *p*-values shown in bold highlight significant differences.

3.3. Respiratory timing variability, apnoeas and sighs during normoxia in behaving rats during quiet rest

Assessments of both short-term (SD1) and long-term (SD2) respiratory timing variability during normoxia were equivalent between groups: T_i (Table 2), T_e ($p > .05$, one-way ANOVA, Fig. 3e, f) and total breath duration (T_{tot} , $p > .05$, Fig. 3g, h). There was no difference in apnoea index (Fig. 3l) or sigh frequency (Fig. 3n) during normoxia between groups ($p > .05$). The apnoea index combines spontaneous and post-sigh apnoeas, both of which were equivalent in their respective prevalences between groups ($p > .05$). Furthermore, the average duration of apnoeas was equivalent between groups (Fig. 3m).

3.4. Ventilatory and metabolic responsiveness to chemostimulation in behaving rats during quiet rest

3.4.1. Ventilatory and metabolic responsiveness to hypoxia

No significant differences were observed between respective groups in ventilatory and metabolic responsiveness to hypoxia determined under steady-state conditions during the last 5 min of exposure (two-way ANOVA, Fig. 2b, c, f, g, j, k, repeated measures two-way ANOVA; Supplementary Fig. 2a, b, e, f, i, j; and Table 3). However, analysis during the first 120 s of hypoxia, when the peak hypoxic ventilatory response was observed, revealed that manipulation of the gut microbiota had a significant effect on minute ventilation due to a decrease in the

respiratory frequency response in ABX rats compared with VEH rats (V_E time, $p = .0001$; ABX, $p = .045$; time x ABX, $p = .459$, two-way ANOVA; f_R time, $p = .0001$; ABX, $p = .022$; time x ABX, $p = .486$, two-way ANOVA, Supplementary Fig. 3a) and in VEH-FMT rats compared with VEH rats (V_E time, $p = .0001$; FMT, $p = .001$; time x FMT, $p = .0009$, two-way ANOVA; f_R time, $p = .0001$; FMT, $p = .002$; time x FMT, $p = .039$, two-way ANOVA, Supplementary Fig. 3c). Ventilatory responses to the AIH protocol were equivalent between respective groups ($p > .05$; Supplementary Fig. 4, Supplementary Table 1).

3.4.2. Ventilatory and metabolic responsiveness to hypercapnia

One of the major findings of this study is that manipulation of the gut microbiota has a significant effect on the ventilatory response to hypercapnia ($p = .02$, Kruskal-Wallis, Table 5). V_E was significantly blunted in ABX rats compared with VEH rats ($p = .038$, two-way ANOVA, Fig. 2h; and $p = .045$; Kruskal-Wallis with Dunn's *post hoc*, Table 5), a consequence of reduced f_R response to CO_2 challenge ($p = .044$, two-way ANOVA, Fig. 2d; and $p = .043$, one-way ANOVA with Bonferroni *post hoc*, Table 5). Further analysis of the f_R response during each minute of the hypercapnic exposure revealed a significant difference in the f_R response to CO_2 challenge in ABX rats compared with VEH rats (time, $p < .0001$; ABX, $p = .047$; time x ABX, $p = .638$, Supplementary Fig. 5a). The hypoventilation was evident as a blunted V_E/VCO_2 response in ABX rats compared with VEH rats, however this was not statistically

Table 2
Baseline ventilation, respiratory timing variability and metabolism in behaving rats during quiet rest.

	VEH (n = 10)	ABX (n = 10)	VEH-FMT (n = 10)	ABX-FMT (n = 10)	One-way ANOVA	VEH vs ABX	VEH-FMT vs ABX-FMT	VEH vs VEH-FMT	ABX vs ABX-FMT	VEH vs ABX-FMT	ABX vs VEH-FMT
f_R (brpm)	83 ± 13	79 ± 11	79 ± 11	79 ± 14	0.845	–	–	–	–	–	–
V_E (ml/min/100 g)	50 ± 6	51 ± 8	48 ± 6	49 ± 7	0.855	–	–	–	–	–	–
V_T (ml/100 g)	0.63 ± 0.07	0.64 ± 0.12	0.61 ± 0.07	0.65 ± 0.06	0.763	–	–	–	–	–	–
V_T/T_i (ml/s/100 g)	2.5 ± 0.4	2.5 ± 0.6	2.5 ± 0.5	2.6 ± 0.4	0.936	–	–	–	–	–	–
T_i (ms)	252 ± 23	264 ± 36	261 ± 26	259 ± 33	0.813	–	–	–	–	–	–
T_e (ms)	537 ± 96	557 ± 86	527 ± 101	565 ± 132	0.844	–	–	–	–	–	–
T_i SD1 (ms)	29 ± 9	24 ± 7	28 ± 11	24 ± 6	0.484	–	–	–	–	–	–
T_i SD2 (ms)	47 ± 20	43 ± 14	50 ± 20	37 ± 11	0.415	–	–	–	–	–	–
VO_2 (ml/min/100 g)	2.7 ± 0.6	3.3 ± 1.0	3.2 ± 0.7	3.0 ± 0.9	0.414	–	–	–	–	–	–
VCO_2 (ml/min/100 g)	1.6 ± 0.3	1.8 ± 0.2	1.8 ± 0.2	1.7 ± 0.3	0.093	–	–	–	–	–	–
V_E/VCO_2	33 ± 6	30 ± 7	27 ± 2	29 ± 3	0.042	0.999	0.999	0.032	0.999	0.437	0.700

f_R , respiratory frequency (brpm, breaths per min); V_E , minute ventilation; V_T , tidal volume; V_T/T_i , mean inspiratory flow; T_i , inspiratory time; T_e , expiratory time; SD1, short-term respiratory timing variability; SD2, long-term respiratory timing variability VO_2 , oxygen consumption; VCO_2 , carbon dioxide production; V_E/VCO_2 , ventilatory equivalent; VEH, autoclaved deionised water; ABX, antibiotic-treated; VEH-FMT, VEH followed by faecal microbiota transfer; ABX-FMT, antibiotic-treated followed by faecal microbiota transfer. Data are shown as mean ± SD and were statistically compared using one-way ANOVA with Bonferroni *post hoc* where appropriate, or non-parametric Kruskal-Wallis test, where appropriate. Each *p*-value is adjusted to account for multiple comparisons. *p*-values shown in bold highlight significant differences.

significant ($p = .093$, two-way ANOVA, Fig. 2l), with values for V_{CO_2} during hypercapnia equivalent between groups (data not shown). Manipulation of the gut microbiota had a significant depressant effect on ventilatory drive to breathe (V_T/T_i) in response to hypercapnic challenge (Table 5). No other ventilatory differences were noted between groups (Supplementary Fig. 5 b–d and Table 5). Repeated measures two-way ANOVA was performed for ventilatory and metabolic responsiveness to hypercapnia revealing that FMT significantly decreased V_E (gas, $p < .0001$; FMT, $p = .014$; gas x FMT, $p = .043$; repeated measures two-way ANOVA, Supplementary Fig. 2g), f_R (gas, $p < .0001$; FMT, $p = .046$; gas x FMT, $p = .103$; repeated measures two-way ANOVA, Supplementary Fig. 2c) and V_E/V_{CO_2} (gas, $p < .0001$; FMT, $p = .003$; gas x FMT, $p = .048$; repeated measures two-way ANOVA, Supplementary Fig. 2k) in VEH-FMT rats compared with VEH rats. Repeated measures two-way ANOVA revealed no difference for V_E , f_R , and V_E/V_{CO_2} in ABX rats compared with ABX-FMT (Supplementary Fig. 2d, h, i). Similarly, no differences were observed for values in ABX-FMT rats compared with VEH-FMT rats (Fig. 2e, l, m; $p > .05$; two-way ANOVA).

3.5. Respiratory timing variability, apnoeas and sighs during hypoxia and hypercapnia in behaving rats during quiet rest

Assessments of short-term (SD1) and long-term (SD2) respiratory timing variability for T_i , T_e and T_{tot} in response to hypoxia (Table 4) and for T_e and T_{tot} in response to hypercapnia (Table 6) were equivalent between groups. T_i SD2 in hypercapnia was altered by microbiota manipulation (Table 6). There was no difference in apnoea index or sigh frequency (Tables 4 and 6) between groups. Furthermore, the average duration of apnoeas during hypercapnia (Table 6) was equivalent between groups.

3.6. Cardiorespiratory recordings in anaesthetised rats

3.6.1. Baseline cardiorespiratory and blood gas parameters

Baseline cardiorespiratory and blood gas measurements in anaesthetised rats are shown in Table 7. There were no significant differences for baseline respiratory parameters between groups. Arterial blood oxygenation, pH and carbon dioxide and bicarbonate concentration were equivalent across groups. Haematocrit and haemoglobin concentrations were significantly lower in ABX rats compared with VEH rats. Manipulation of the gut microbiota lowered systolic blood pressure (Table 7). *Post hoc* analysis revealed that systolic blood pressure was significantly lower in ABX rats compared with VEH, VEH-FMT and ABX-FMT rats but no difference in mean arterial blood pressure was observed between groups (Table 7).

3.6.2. Cardiorespiratory responses to 5-HT₃ receptor agonism evoking the cardiopulmonary reflex

Stimulation, using PBG, of 5-HT₃ receptors found on pulmonary vagal afferent nerves evoked the integrated cardiopulmonary reflex with no significant difference in apnoea duration in ABX rats compared with VEH rats ($p > .05$, two-way ANOVA, Fig. 4b), or in ABX-FMT rats compared with VEH-FMT rats ($p > .05$, two-way ANOVA, Fig. 4f). A similar outcome was determined for post-apnoea induced tachypnoeic episodes in ABX rats compared with VEH rats ($p > .05$, two-way ANOVA, Fig. 4c), and ABX-FMT rats compared with VEH-FMT rats ($p > .05$, two-way ANOVA, Fig. 4g). The depressor response to PBG administration (hypotension) and bradycardia were also equivalent between ABX rats and VEH rats ($p > .05$, two-way ANOVA, Fig. 4d, e) and in ABX-FMT rats compared with VEH-FMT rats ($p > .05$, two-way ANOVA, Fig. 4h, i). The cardiorespiratory responses to high-dose PBG were abolished following bilateral cervical vagotomy.

3.7. Brainstem neurochemistry

L -DOPA, DA, HVA, HVA/DA ratio, 5-HT and 5-HIAA concentrations in the brainstem were significantly affected by manipulation of the gut microbiota ($p < .05$; one-way ANOVA or Kruskal-Wallis, Fig. 5). Additionally, *post hoc* analysis revealed that compared with VEH, ABX brainstem homogenates contained elevated concentrations of L -DOPA ($p = .009$; Kruskal-Wallis with Dunn's *post hoc*, Fig. 5a) and an increased HVA/DA ratio ($p = .0001$; one-way ANOVA with Bonferroni *post hoc*, Fig. 5d), a consequence of augmented HVA concentrations ($p < .0001$, one-way ANOVA with Bonferroni *post hoc*, Fig. 5c) and decreased DA concentrations ($p = .025$; one-way ANOVA with Bonferroni *post hoc*, Fig. 5b). ABX-FMT samples compared with VEH, ABX and VEH-FMT brainstem homogenates had significant increases in HVA/DA ratio ($p < .0001$; $p = .001$; $p = .0001$, respectively; one-way ANOVA with Bonferroni *post hoc*, Fig. 5d) due to elevated HVA concentrations ($p < .0001$; $p = .003$; $p = .0002$, respectively; one-way ANOVA with Bonferroni *post hoc*, Fig. 5c). L -DOPA was elevated in ABX-FMT rats compared with VEH and VEH-FMT brainstem homogenates ($p = .001$; $p = .038$, respectively, Kruskal-Wallis with Dunn's *post hoc*, Fig. 5a). Furthermore, ABX-FMT contained increased concentrations compared with VEH of 5-HT ($p = .021$; one-way ANOVA with Bonferroni *post hoc*, Fig. 5f) and 5-HIAA ($p = .01$; one-way ANOVA with Bonferroni *post hoc*, Fig. 5g) along with a decrease in DA concentration ($p = .0009$; one-way ANOVA with Bonferroni *post hoc*, Fig. 5b). VEH-FMT brainstem homogenates compared with VEH had elevated HVA/DA ratio ($p = .0005$; one-way ANOVA with Bonferroni *post hoc*, Fig. 5d) due to an increase in HVA ($p = .0004$; one-way ANOVA with Bonferroni *post hoc*, Fig. 5c).

3.8. Ex vivo intestinal macromolecular permeability

The distal ileum from ABX rats was significantly more permeable compared with VEH rats: FITC flux was enhanced in ABX tissue compared with VEH at the 120-min time point ($p = .025$, two-way ANOVA with Bonferroni *post-hoc*, Fig. 7a). However, no statistically significant difference was detected in the permeability of the proximal colon of ABX rats compared with VEH rats ($p > .05$; Fig. 7c). Permeability was equivalent in both the distal ileum and proximal colon of ABX-FMT rats compared with VEH-FMT rats ($p > .05$; Fig. 7b, d). Permeability of the distal ileum, but not proximal colon, was increased in VEH-FMT compared with VEH (Supplementary Fig. 6).

3.9. Alterations in the caecal microbiota

As expected, ABX rats had a significantly heavier caecum compared with VEH rats ($p = .002$; Kruskal-Wallis with Dunn's *post hoc*, Fig. 6d). Faecal microbiota transfer attenuated the effects of antibiotics on caecum weight; ABX-FMT and VEH-FMT rat caecum weights were lighter compared with ABX ($p = .0001$ and $p = .03$, respectively; Kruskal-Wallis with Dunn's *post hoc*, Fig. 6d). DNA concentrations in caecal samples from ABX rats were critically low, likely a result of depletion of bacteria by the broad-spectrum antibiotic cocktail and thus below the level of detection. This prevented a comparative analysis of microbiota composition and diversity as 16S rRNA sequencing was not possible in this group. In the remaining groups, 16S rRNA sequencing identified around 130 bacterial genera from 46 families of 9 different phyla (Supplementary Tables 14–22). The majority of the bacterial genera belonged to two major phyla (Bacteroidetes and Firmicutes), which together comprise 95% (VEH), 90% (VEH-FMT) and 85% (ABX-FMT) of intestinal microbiota. The analysis of alpha and beta diversities revealed that FMT procedure significantly altered the microbiota composition in both VEH-FMT and ABX-FMT rats as compared with VEH rats. There was a clear trend towards enhanced species richness of caecal microbiota in VEH-FMT and ABX-FMT samples: number of observed species, Chao1 (an estimate of total richness in a sample [48]) and phylogenetic whole tree diversity (PD whole tree, an estimate of diversity based on structure and branch

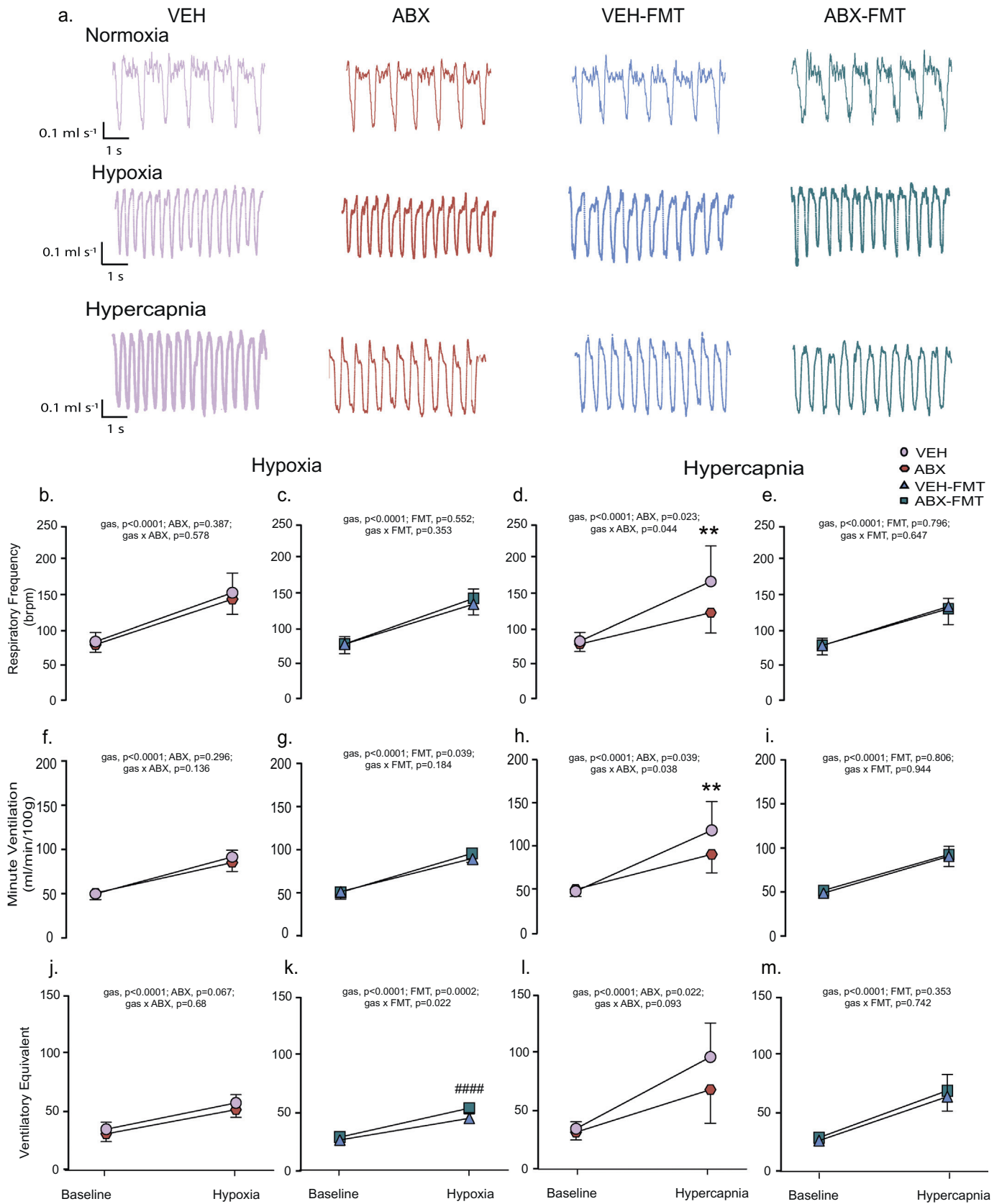


Fig. 2. Chronic antibiotic administration and faecal microbiota transfer blunts hypercapnic ventilation in behaving rats during quiet rest. a) Representative traces of typical respiratory flow during normoxic, hypoxic and hypercapnic ventilation in VEH, ABX, VEH-FMT and ABX-FMT rats; downward deflections represent inspiration. Group data for respiratory frequency (b, c, d, e), minute ventilation (f, g, h, i) and ventilatory equivalent (j, k, l, m) during normoxia and in response to hypoxia (b, c, f, g, j, k) and hypercapnia (d, e, h, i, l, m) for VEH and ABX (b, f, j, d, h, l) and VEH-FMT and ABX-FMT (c, g, k, e, i, m). VEH, autoclaved deionised water; ABX, antibiotic-treated; VEH-FMT, VEH followed by faecal microbiota transfer; ABX-FMT, antibiotic-treated followed by faecal microbiota transfer. Data (b-m) are expressed as mean \pm SD during baseline, hypoxia and hypercapnia; $n = 10$ for all groups. Groups were statistically compared by two-way ANOVA with Bonferroni *post hoc* where appropriate. P values are shown. ** $p < .01$, ABX versus VEH, Bonferroni *post hoc* test.

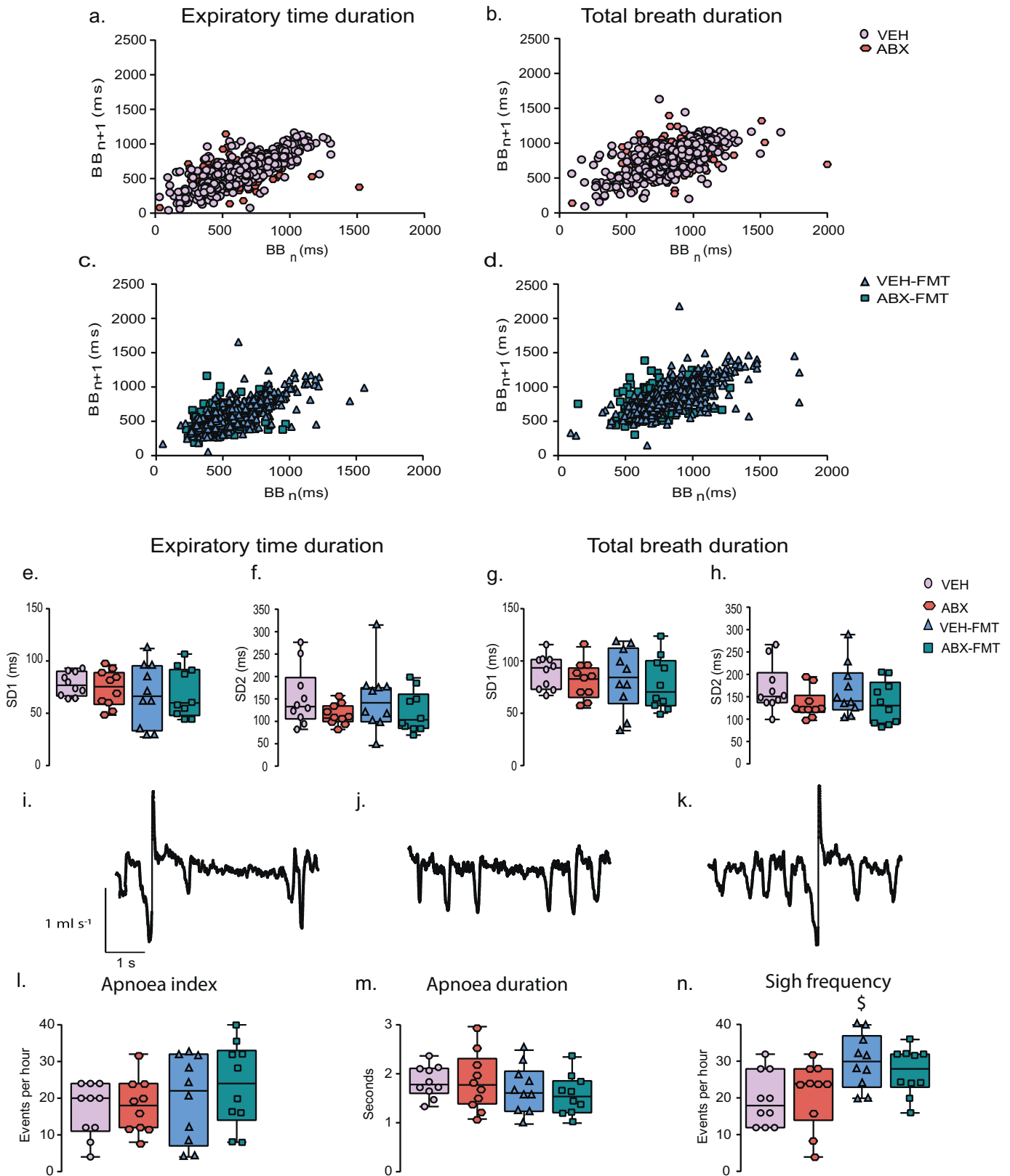


Fig. 3. Chronic antibiotic administration and faecal microbiota transfer do not alter respiratory timing variability, or the prevalence of apnoeas and sighs in behaving rats during quiet rest. Poincaré plots of breath-to-breath (BB_n) and subsequent breath-to-breath (BB_{n+1}) interval of expiratory duration (T_e ; a, c) and total breath duration (T_{tot} ; b, d) for 200 consecutive breaths for VEH and ABX (a, b) and VEH-FMT and ABX-FMT rats (c, d). Group data for T_e short-term variability (SD1; e) and long-term variability (SD2; f) and T_{tot} SD1 (g) and SD2 (h) in VEH, ABX, VEH-FMT and ABX-FMT rats during normoxia. Representative respiratory flow traces (downward deflections represent inspiration) illustrating a spontaneous sigh followed by an apnoea (i), a spontaneous apnoea (j) and a spontaneous sigh (k). Group data of apnoea index (l), apnoea duration (m) and sigh frequency (n). VEH, autoclaved deionised water; ABX, antibiotic-treated; VEH-FMT, VEH followed by faecal microbiota transfer; ABX-FMT, antibiotic-treated followed by faecal microbiota transfer. Groups (e–h, l–n) are expressed as box and whisker plots (median, IQR and minimum to maximum values); $n = 10$ for all groups. Groups were statistically compared by one-way ANOVA or non-parametric Kruskal-Wallis with Dunn's *post hoc*, where appropriate. § $p < .05$, VEH-FMT versus VEH, Dunn's *post hoc* test.

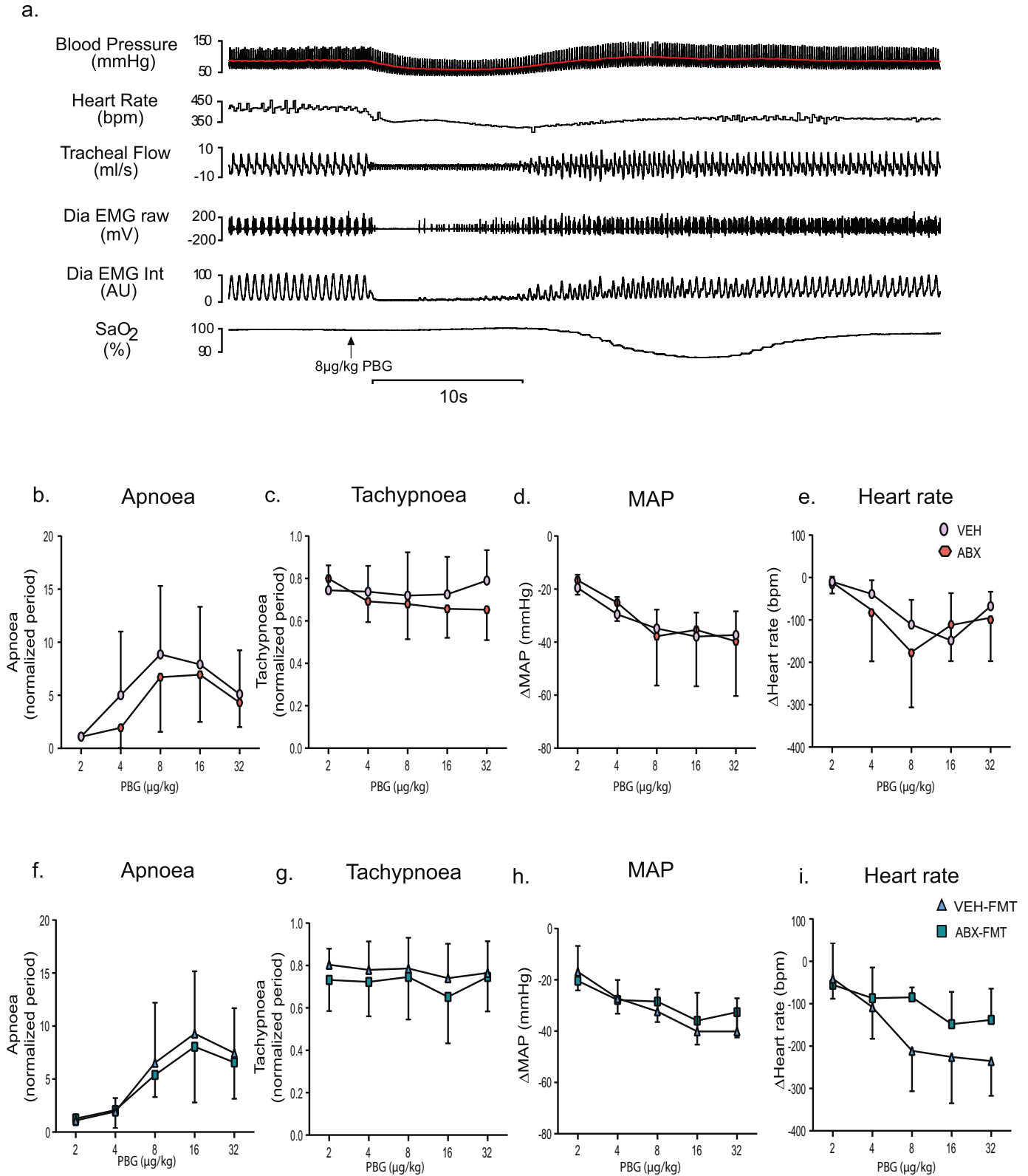


Fig. 4. Chronic antibiotic administration and faecal microbiota transfer do not alter cardiorespiratory responses to phenylbiguanide administration in anaesthetised rats. a) Representative traces of blood pressure (red indicates mean value), heart rate, tracheal airflow, raw and integrated diaphragm (Dia) electromyogram (EMG) activity and arterial oxygen saturation (SaO₂) during intravenous administration of 5-HT₃ agonist phenylbiguanide (PBG; 8 μg/kg) indicated by the upwards arrow. Group data for maximum apnoea duration (b, f) and tachypnoea (c, g) normalised to baseline respiratory period in response to 2, 4, 8, 16 and 32 μg/kg of PBG for VEH and ABX (b, c) and for VEH-FMT and ABX-FMT rats (f, g). Absolute change in mean arterial blood pressure (MAP; d, h) and heart rate (e, i) in response to 2, 4, 8, 16 and 32 μg/kg of PBG for VEH and ABX (d, e) and for VEH-FMT and ABX-FMT rats (h, i). VEH, autoclaved deionised water; ABX, antibiotic-treated; VEH-FMT, VEH followed by faecal microbiota transfer; ABX-FMT, antibiotic-treated followed by faecal microbiota transfer. Data (b-i) are expressed mean ± SD; VEH (n = 8), ABX (n = 8), VEH-FMT (n = 9) and ABX-FMT (n = 10). Groups were statistically compared by two-way ANOVA for VEH and ABX and separately for VEH-FMT and ABX-FMT.

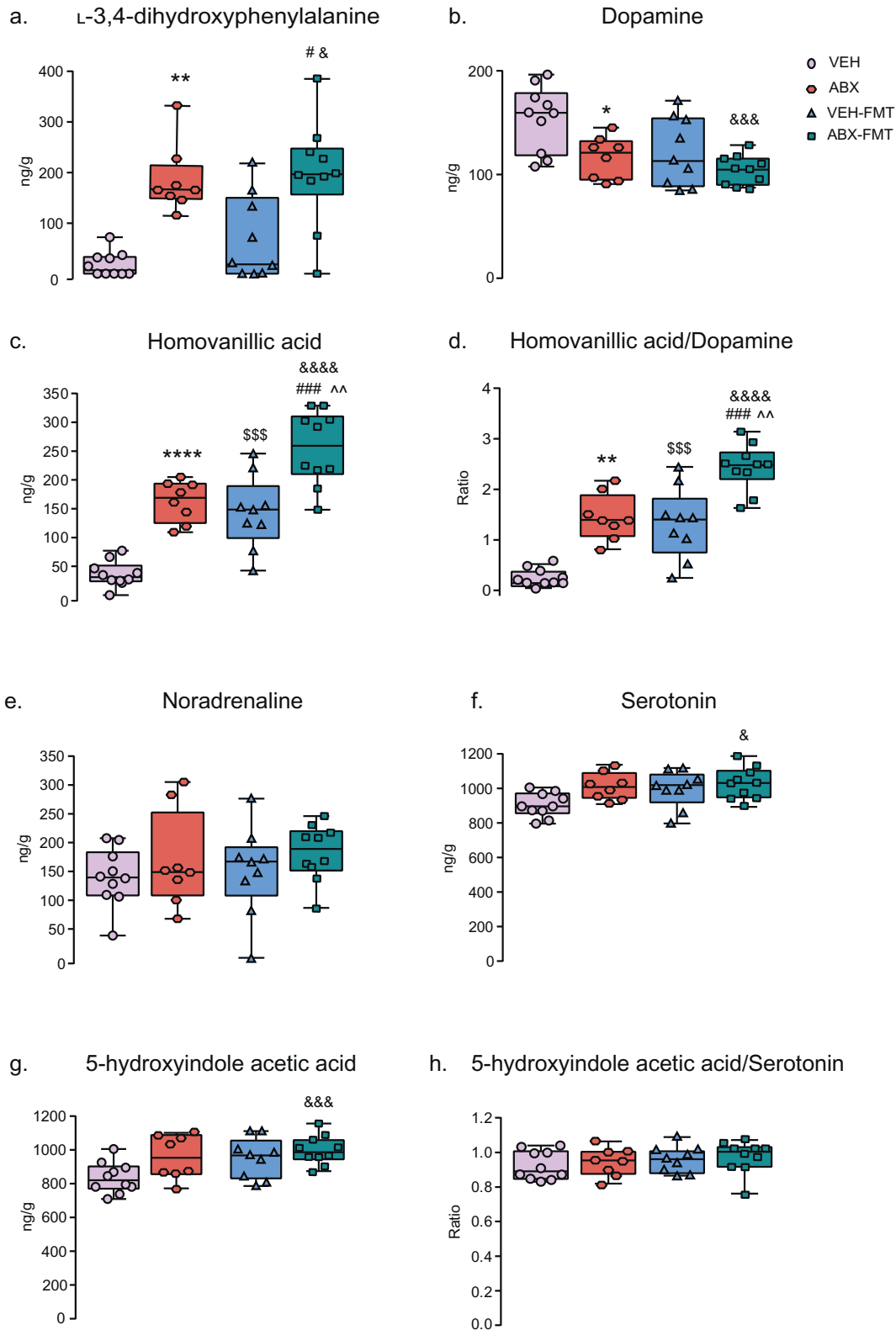


Fig. 5. Chronic antibiotic administration and faecal microbiota transfer alter rat brainstem neurochemistry. Group data for L-3,4-dihydroxyphenylalanine (a), dopamine (b), homovanillic acid (c), homovanillic acid/dopamine ratio (d), noradrenaline (e), serotonin (f), 5-hydroxyindole acetic acid (g) and 5-hydroxyindole acetic acid/serotonin ratio (h) in VEH, ABX, VEH-FMT and ABX-FMT rats. VEH, autoclaved deionised water; ABX, antibiotic-treated; VEH-FMT, VEH followed by faecal microbiota transfer; ABX-FMT, antibiotic-treated followed by faecal microbiota transfer. Data (a-h) are expressed as box and whisker plots (median, IQR and minimum to maximum values). VEH ($n = 10$), ABX ($n = 8$), VEH-FMT ($n = 9$) and ABX-FMT ($n = 10$). Groups were statistically compared by one-way ANOVA with Bonferroni *post hoc* or non-parametric Kruskal-Wallis with Dunn's *post hoc*, where appropriate. * $p < .05$, ** $p < .01$, **** $p < .0001$, ABX versus VEH; \$ $p < .05$, \$\$\$ $p < .001$, VEH versus VEH-FMT; & $p < .05$, &&& $p < .001$, &&&& $p < .0001$, VEH versus ABX-FMT; # $p < .05$, ### $p < .001$, VEH-FMT versus ABX-FMT; ^^ $p < .01$, ABX versus ABX-FMT; all *post hoc* tests.

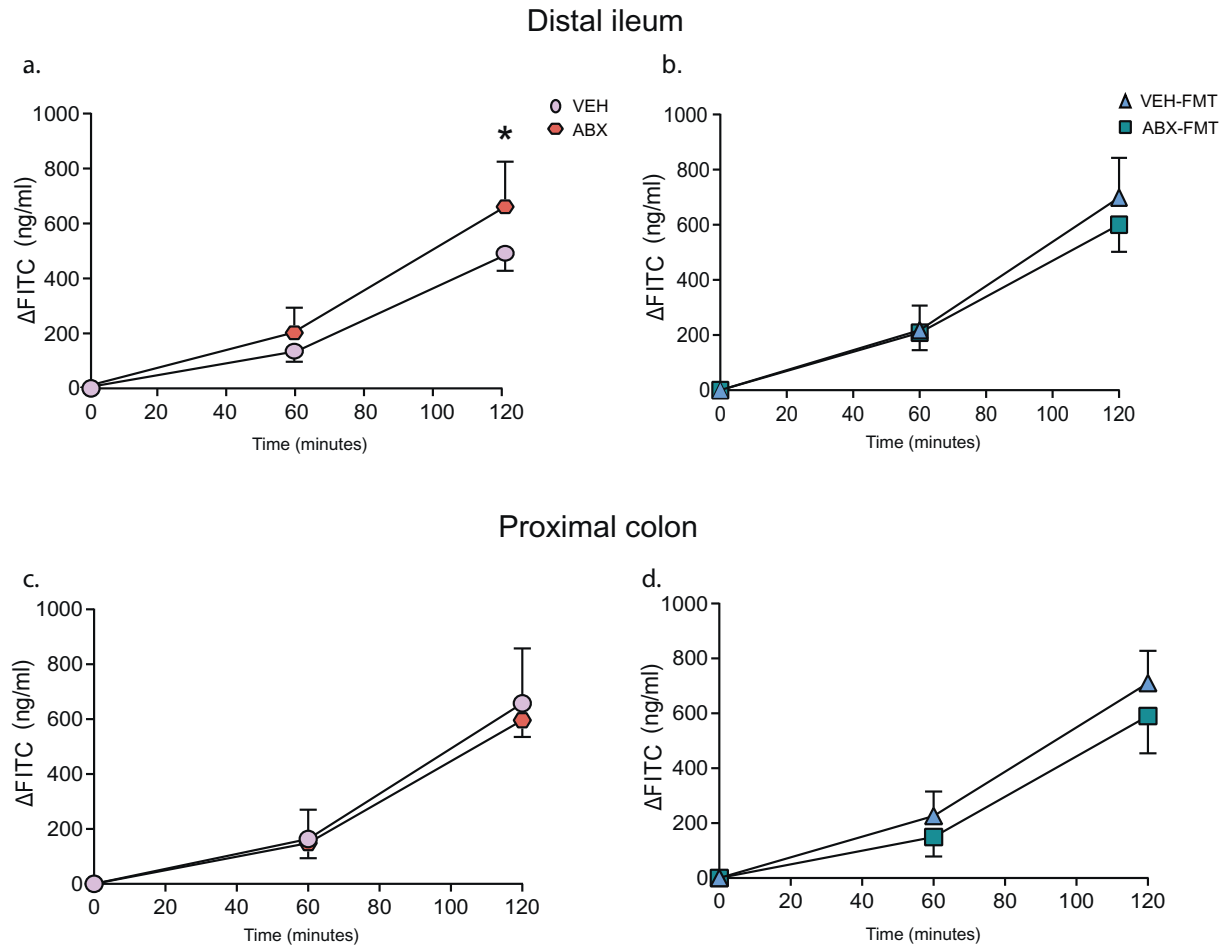


Fig. 6. Chronic antibiotic administration increases the macromolecular permeability of rat distal ileum. Group data for FITC flux in distal ileum (a, b) and proximal colon (c, d) in VEH and ABX (a, c) and in VEH-FMT and ABX-FMT rats (b, d). VEH, autoclaved deionised water; ABX, antibiotic-treated; VEH-FMT, VEH followed by faecal microbiota transfer; ABX-FMT, antibiotic-treated followed by faecal microbiota transfer. Groups (a–d) showing baseline (0 min), 60 min and 120 min FITC flux for VEH ($n = 4–5$), ABX ($n = 6$), VEH-FMT ($n = 5$) and ABX-FMT ($n = 4$). Groups were statistically compared by two-way ANOVA with Bonferroni *post hoc*, where appropriate. * $p < .05$, ABX versus VEH.

length of the phylogenetic tree in each sample [49]) indices were all increased in these groups (Fig. 7a, $p = .035$, $p = .043$ and $p = .004$ between VEH-FMT versus VEH; $p = .052$ for parameters in ABX-FMT versus VEH). However, only an increase in PD whole tree diversity in VEH-FMT vs. VEH rats remained significant after adjustment for multiple comparisons. Shannon and Simpson metrics of alpha diversity, which take into account the evenness of species abundance, were less affected by FMT. Further, PCoA analysis identified structural differences across all three groups, with VEH-FMT and ABX-FMT rats clearly separating from VEH rats (Fig. 7b, $p = .001$, PERMANOVA).

At the phyla level, VEH-FMT and ABX-FMT rat caecal contents displayed a distinct shift towards an increase in Proteobacteria and Cyanobacteria with a decrease in Bacteroidetes and Deferribacteres compared with VEH rats (Supplementary Tables 14 and 15). Five minor phyla remained unchanged between VEH-FMT and ABX-FMT rats compared with VEH rats (Supplementary Tables 14 and 15). The minor phyla Verrucomicrobia and Saccharibacteria were significantly altered in ABX-FMT rats compared with VEH-FMT rats (Supplementary Table 16).

An increase in the relative abundance of Proteobacteria in VEH-FMT and ABX-FMT rats was primarily caused by a shift in *Helicobacter* bacteria, a genus of *Helicobacteraceae* family (Fig. 7c). Increased abundance of *Helicobacter* in VEH-FMT rats compared with VEH rats appeared to be at the expense of *Parasutterella* (*Alcaligenaceae*) and *Enterobacter* (*Enterobacteriaceae*), which both displayed a reduced relative abundance. The Cyanobacteria shifts evident in VEH-FMT and ABX-FMT rats were attributed to an increase in *Gastranaerophilales* uncultured species.

Bacteroidales S24–7 uncultured bacteria, a dominant genus of S24–7 family, was the main source of Bacteroidetes reduction in VEH-FMT rat caecal samples compared with VEH rats; nonetheless, an increase in minor Bacteroidetes V2.1 *Bac22* uncultured species was noted (Fig. 7c). The decrease in Bacteroidetes in the ABX-FMT rats was not related to a compelling decrease in any one genus but rather small shifts in the relative abundance of multiple genera. Similar to the VEH-FMT group, a minor increase in Bacteroidetes V2.1 *Bac22* uncultured bacterium was detected in ABX-FMT rats. The decrease in Deferribacteres in VEH-FMT and ABX-FMT rats compared with VEH rats was a consequence of a decrease in *Mucispirillum* (*Deferribacteraceae* family). Although there was no significant difference at the Firmicutes phylum level, VEH-FMT rats showed an increase in uncultured bacterium and unidentified genera from *Clostridiales* vadin BB60 family, *Lachnoclostridium-10*, *Lachnospiraceae* uncultured, *Flavonifractor*, *Ruminococcaceae* UCG-013 compared with VEH. A decrease occurred in *Bacillus*, *Lachnospiraceae* UCG-008, *Tyzzereella* and *Ruminoclostridium-9* (Fig. 7c). In ABX-FMT rats there was an increase in *Lachnoclostridium-10* and *Ruminococcaceae* UCG-011 and a decrease in *Bacillus*, *Streptococcus* and *Lachnospiraceae* UCG-008 compared with VEH rats. Furthermore, uncultured *Coriobacteriaceae* bacteria from the Actinobacteria phylum was reduced in the VEH-FMT and ABX-FMT rats compared with VEH rats. The alterations evident at phyla level in ABX-FMT rats compared with VEH-FMT rats were not related to changes in highly abundant genera. Nonetheless, there was a decrease in *Streptococcus* (*Streptococcaceae*), *Peptoclostridium* (*Peptococcaceae*), *Ruminococcaceae* UCG-005

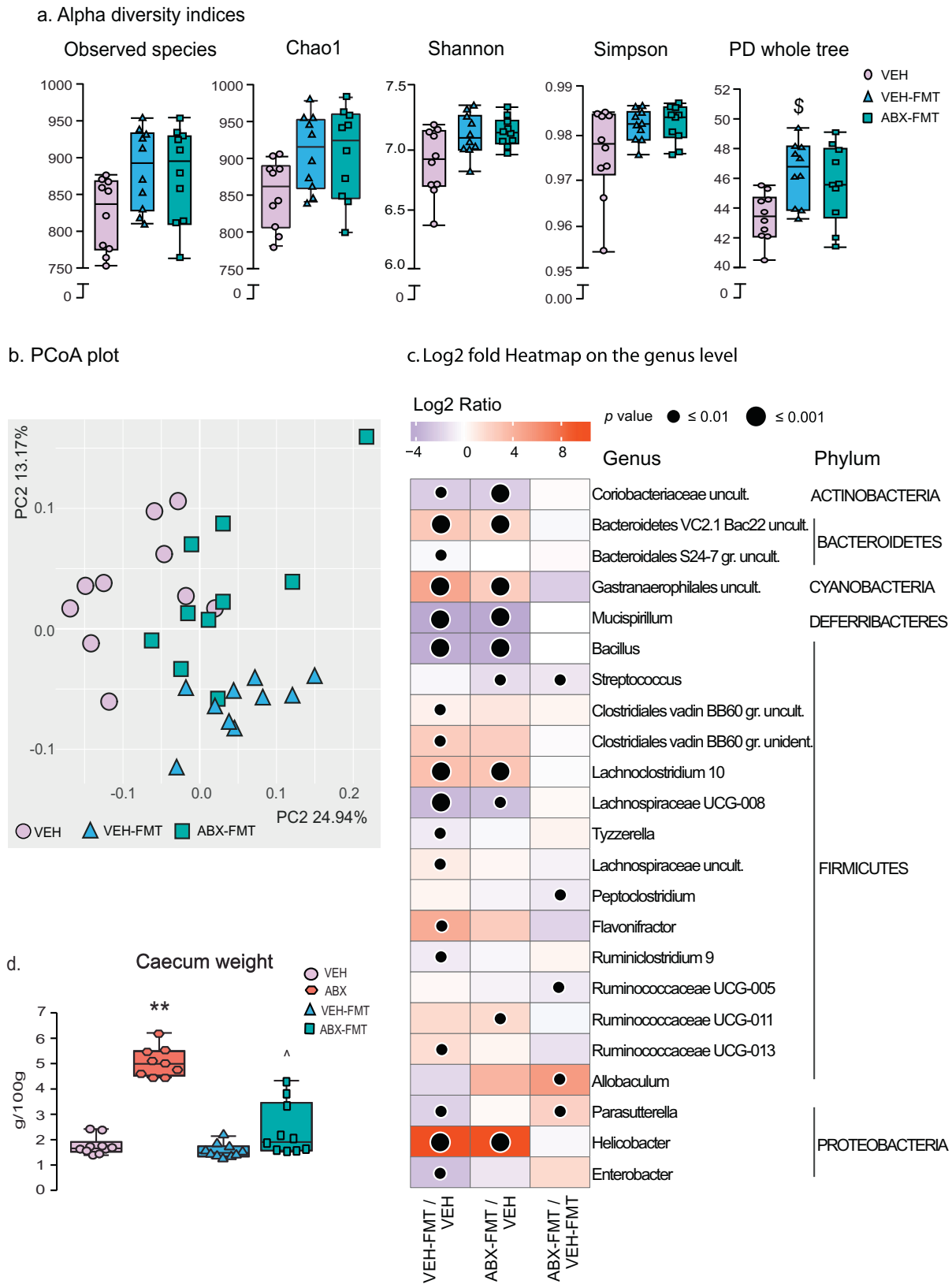


Fig. 7. Faecal microbiota transfer alters rat caecal microbiota composition. Group data for alpha diversity (a) and principal coordinate analysis (PCoA; b) in 2-dimensional representations for VEH, VEH-FMT and ABX-FMT. Heatmap of Log2 fold change ratios on genus level (c) showing increases (red) and decreases (purple) in the relative abundance of bacterial genera in VEH-FMT (left column) and ABX-FMT (middle column) compared with VEH, as well as differences between ABX-FMT and VEH-FMT (right column). Group (d) data for caecum weight in VEH, ABX, VEH-FMT and ABX-FMT. VEH, autoclaved deionised water; VEH-FMT, VEH followed by faecal microbiota transfer; ABX-FMT, antibiotic-treated followed by faecal microbiota transfer. Data (a and d) are expressed as box and whisker plots (median, IQR and minimum to maximum values). Data (a) were statistically compared by non-parametric Mann-Whitney U test. Group (d) were statistically compared by Kruskal-Wallis with Dunn's *post hoc*. ***p* < .01, ABX versus VEH; €€€€ *p* < .0001, VEH-FMT vs ABX; ^ *p* < .05, ABX-FMT vs. ABX. c) ● *p* < .05, ● *p* < .01, ● *p* < .001 compared with VEH or VEH-FMT values. Benjamini-Hochberg adjustment with *Q* = 0.1 was used to correct *p* values for multiple testing; VEH (*n* = 10), VEH-FMT (*n* = 10) and ABX-FMT (*n* = 10).

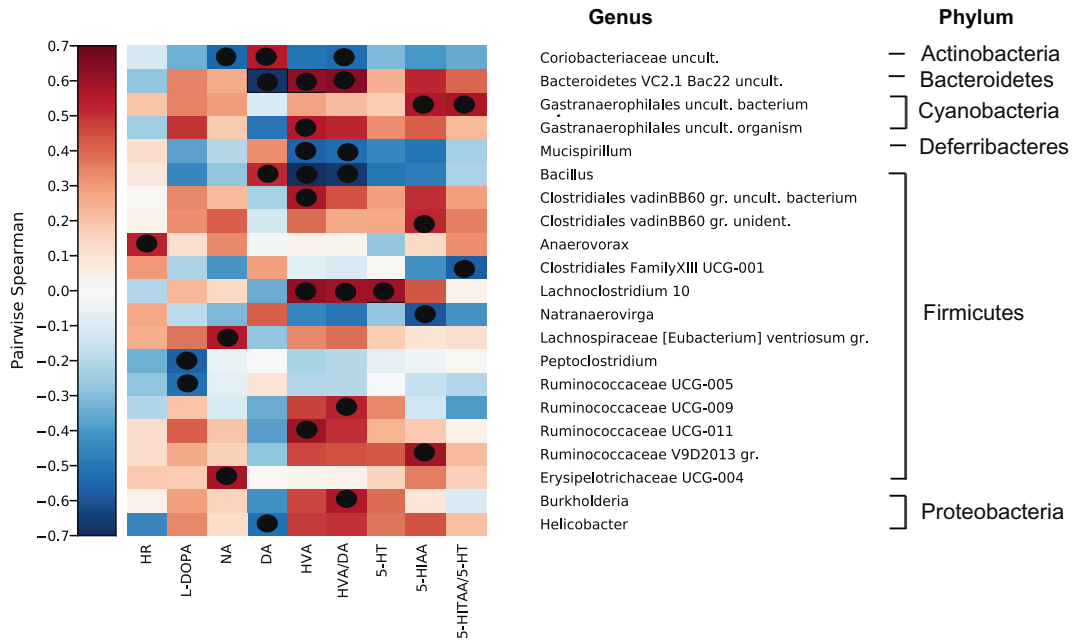


Fig. 8. Brainstem neurochemistry and heart rate are associated with the abundance of specific genera. Hallagram depicting Spearman correlations between the relative abundance of bacterial genera and brainstem neurochemistry as well as basal heart rate (VEH, VEH-FMT and ABX-FMT). Genera are ordered taxonomically. HR, heart rate; L-DOPA, L-3,4-dihydroxyphenylalanine; NA, noradrenaline; DA, dopamine; HVA, homovanillic acid; HVA/DA, homovanillic acid/dopamine; 5-HT, serotonin; 5-HIAA, 5-hydroindole acetic acid; 5-HITAA/5-HT, 5-hydroindole acetic acid/serotonin. Significant correlations are represented by black dots (●). Benjamini-Hochberg adjustment *p*-value with *Q* = 0.2 was used to correct *p* values for multiple testing.

(*Ruminococcaceae*) compared with VEH-FMT rats. ABX-FMT rats displayed an increase in *Allobaculum* (*Erysipelotrichaceae*) and *Parasutterella* (*Alcaligenaceae*) from the phyla Firmicutes and Proteobacteria, respectively (Fig. 7c).

3.10. Correlation analysis between microbiota composition and brainstem neurochemistry and heart rate

Associations between genera and brainstem neurochemistry as well as basal heart rate in VEH, VEH-FMT and ABX-FMT rats were identified utilising Hierarchical All-against-All (HALLA) correlation analysis. Identified associations are presented as a correlogram in Fig. 8. Individual data points for the most significant correlations for homovanillic, homovanillic/dopamine and dopamine are presented as scatter plots in Supplementary Fig. 7. *Anaerovorax*, a member of Firmicutes phylum positively associated with basal heart rate. Further to this, several genera from different phyla correlated with brainstem neurochemistry. *Peptoclostridium* and *Ruminococcaceae* UCG-005 of Firmicutes phylum negatively associated with L-DOPA. *Lachnospiraceae* (*Eubacterium*)

ventriosum group and *Erysipelotrichaceae* UCG-004 of Firmicutes positively associated with NA, while *Coriobacteriaceae* uncultured, a genus of Actinobacteria negatively associated with NA. *Helicobacter*, a member of Proteobacteria phylum as well as *Bacteroidetes* VC2.1 Bac22 uncultured, a member of Bacteroidetes phylum negatively correlated with DA. *Bacillus*, of Firmicutes phylum and *Coriobacteriaceae* uncultured positively correlated with DA. *Bacteroidetes* VC2.1 Bac22 uncultured *Gastranaerophilales* uncultured organism as well as 3 genera from Firmicutes phylum, *Ruminococcaceae* UCG-011, *Lachnoclostridium* 10 and *Clostridiales vadin BB60* group uncultured bacterium positively associated with HVA, whereas *Bacillus* and *Mucispirillum*, a member of Deferribacteres phylum negatively associated with HVA. *Ruminococcaceae* UCG-009, *Lachnoclostridium* 10, *Bacteroidetes* VC2.1 Bac22 uncultured and *Burkholderia*, a member of phylum Proteobacteria positively associated with HVA/DA turnover. *Bacillus*, *Mucispirillum* and *Coriobacteriaceae* uncultured negatively associated with this ratio. *Lachnoclostridium* 10 positively correlated with 5-HT. *Ruminococcaceae* V9D2013 group, *Clostridiales vadinBB60* group uncultured bacterium, *Gastranaerophilales* uncultured bacterium and *Bacteroidetes* VC2.1

Table 3
Ventilatory and metabolic responsiveness during hypoxia in behaving rats during quiet rest.

	VEH (n = 10)	ABX (n = 10)	VEH-FMT (n = 10)	ABX-FMT (n = 10)	One-way ANOVA
Δf_R (brpm)	68 ± 20	63 ± 20	57 ± 21	65 ± 17	0.585
ΔV_E (ml/min/100 g)	43 ± 8	36 ± 14	36 ± 9	43 ± 13	0.244
ΔV_T (ml/100 g)	0.07 ± 0.08	0.06 ± 0.08	0.08 ± 0.06	0.02 ± 0.08	0.35
$\Delta V_T/T_i$ (ml/s/100 g)	4.4 ± 0.7	4.1 ± 1.1	3.6 ± 0.7	4.1 ± 0.6	0.168
ΔT_i (ms)	-87 ± 28	-95 ± 41	-87 ± 32	-92 ± 34	0.933
ΔT_e (ms)	-236 ± 62	-239 ± 78	-208 ± 72	-263 ± 106	0.153
ΔVO_2 (ml/min/100 g)	-1.0 ± 0.7	-1.4 ± 1.1	-0.9 ± 0.8	-0.86 ± 0.9	0.522
ΔVCO_2 (ml/min/100 g)	0.2 ± 0.5	-0.005 ± 0.3	0.09 ± 0.2	0.02 ± 0.2	0.444
$\Delta V_E/VCO_2$	22 ± 10	20 ± 9	18 ± 6	24 ± 5	0.335

f_R , respiratory frequency (brpm, breaths per min); V_E , minute ventilation; V_T , tidal volume; V_T/T_i , mean inspiratory flow; T_i , inspiratory time; T_e , expiratory time; SD1, short-term respiratory timing variability; SD2, long-term respiratory timing variability VO_2 , oxygen consumption; VCO_2 , carbon dioxide production; V_E/VCO_2 , ventilatory equivalent; VEH, autoclaved deionised water; ABX, antibiotic-treated; VEH-FMT, VEH followed by faecal microbiota transfer; ABX-FMT, antibiotic-treated followed by faecal microbiota transfer. Data are shown as mean ± SD and were statistically compared using one-way ANOVA with Bonferroni *post hoc* where appropriate. Each *p*-value is adjusted to account for multiple comparisons. Data are expressed as absolute change from baseline (Δ parameter).

Table 4
Respiratory timing variability, apnoeas and sighs during hypoxia in behaving rats during quiet rest.

	VEH (n = 10)	ABX (n = 10)	VEH-FMT (n = 10)	ABX-FMT (n = 10)	One-way ANOVA
T _i SD1 (ms)	28 ± 5	30 ± 6	30 ± 6	29 ± 7	0.744
T _i SD2 (ms)	57 ± 10	67 ± 19	59 ± 9	57 ± 16	0.272
T _e SD1 (ms)	79 ± 28	89 ± 35	77 ± 15	80 ± 31	0.804
T _e SD2 (ms)	140 ± 27	147 ± 32	132 ± 37	130 ± 42	0.699
T _{tot} SD1 (ms)	102 ± 31	112 ± 38	99 ± 15	102 ± 33	0.803
T _{tot} SD2 (ms)	217 ± 30	237 ± 35	217 ± 32	203 ± 64	0.405
Apnoea index (events/h)	0.6 ± 1.9	3.0 ± 4.2	1.2 ± 2.5	1.2 ± 2.5	0.398
Sigh frequency (events/h)	148 ± 35	166 ± 71	172 ± 46	160 ± 29	0.715

T_i, inspiratory time; T_e, expiratory time; T_{tot}, total breath duration; SD1, short-term respiratory timing variability; SD2, long-term respiratory timing variability; VEH, autoclaved deionised water; ABX, antibiotic-treated; VEH-FMT, VEH followed by faecal microbiota transfer; ABX-FMT, antibiotic-treated followed by faecal microbiota transfer. Data are shown as mean ± SD and were statistically compared using one-way ANOVA or non-parametric Kruskal-Wallis test where appropriate.

Bac22 uncultured, positively correlated with 5-HIAA. *Natranaerovirga* negatively associated with 5-HIAA. *Clostridiales Family XII UCG-001* negatively associated with 5HIAA/5-HT.

4. Discussion

There is considerable interest in the role of the gut microbiota in health and disease. This interest stems from established associations between the gut microbiota and brain behaviours [5,6,50–53]. Our interests relate to the potential influence of the microbiota on the cardiorespiratory system. We sought to assess the effects of manipulation of the gut microbiota by chronic antibiotic administration on cardiorespiratory physiology in adult male rats, and to investigate if faecal microbiota transfer of pooled control faeces could reverse or ameliorate putative deleterious effects induced by chronic antibiotic administration (microbiota disruption). The principal findings of this study are: 1) ABX and FMT blunt the ventilatory response to hypercapnia due to decreased respiratory frequency; 2) ABX and FMT blunt respiratory frequency during the peak hypoxic ventilatory response; 3) neither ABX nor FMT interventions alter respiratory timing variability; 4) ABX decreases systolic blood pressure; 5) cardiorespiratory responsiveness to vagal afferent nerve stimulation is unaffected by ABX or FMT; 6) ABX and FMT alter brainstem monoamine and monoamine metabolite concentrations; 7) ABX and FMT, increases distal ileum permeability; 8) FMT significantly altered gut microbiota composition and diversity; 9) Genera from 6 phyla, predominantly Firmicutes, correlate with brainstem neurochemistry.

4.1. Animal model

4.1.1. Microbiota manipulation by chronic antibiotic administration

Two different approaches were used in this study to manipulate the microbiota. First, we used an antibiotic cocktail, informed by previous

studies where microbiota depletion was successful [5,36]. Failure to determine the caecal microbiota composition of ABX rats in the current study was likely the result of severe microbiota depletion and substantially diminished available bacterial DNA for detection. This was further supported by the dramatic enlargement of the caecum in ABX rats; an increase in caecum mass results from the loss of bacterial fermentation, consistent with previous observations both in germ-free and antibiotic-treated animals [54,55]. Faecal output in ABX rats was qualitatively determined as having an increased water composition, a frequent complication of antibiotic administration [55]. We postulate that altered defaecation may have resulted from antibiotic-induced microbiota depletion and potential expansion of opportunistic bacteria [56].

4.1.2. Faecal microbiota transfer significantly altered gut microbiota composition and diversity

In addition to ABX, we utilised a FMT strategy to manipulate gut microbiota. It has been shown that behavioural phenotypes can be transferred via FMT in rodents [5,57–59]. The FMT strategy used in our study did not recover or normalise the microbiota composition. VEH-FMT and ABX-FMT groups both displayed profound changes in microbiota structure and species diversity compared with the VEH group. Caecal samples from VEH-FMT and ABX-FMT animals had the relative abundance of 18 and 10 genera altered, respectively, compared with VEH animals. Only 5 genera were significantly different between VEH-FMT and ABX-FMT. Our findings are consistent with recent clinical data where FMT to persons with irritable bowel syndrome led to the establishment of unique taxonomy as well as increased diversity with no improvement in symptoms [60]. Pooled exogenous bacteria has been shown to increase microbiota diversity in recipient rats, resembling that of the donor [61]. However, pre-treatment with antibiotics does not facilitate establishment of the donor microbiota [61]. Interestingly, autologous FMT had no effect on insulin sensitivity in obese metabolic syndrome,

Table 5
Ventilatory and metabolic responsiveness during hypercapnia in behaving rats during quiet rest.

	VEH (n = 10)	ABX (n = 10)	VEH-FMT (n = 10)	ABX-FMT (n = 10)	One-way ANOVA	VEH vs ABX	VEH-FMT vs ABX-FMT	VEH vs VEH-FMT	ABX vs ABX-FMT	VEH vs ABX-FMT	ABX vs VEH-FMT
Δf _R (brpm)	86 ± 52	45 ± 29	56 ± 15	53 ± 18	0.038	0.043	0.999	0.281	0.999	0.164	0.999
ΔV _E (ml/min/100 g)	67 ± 33	39 ± 23	42 ± 15	42 ± 14	0.02	0.045	0.999	0.091	0.999	0.066	0.999
ΔV _T (ml/100 g)	0.15 ± 0.12	0.11 ± 0.16	0.08 ± 0.07	0.07 ± 0.06	0.33	–	–	–	–	–	–
ΔV _T /T _i (ml/s/100 g)	4.7 ± 1.6	3.1 ± 1.3	2.9 ± 1.0	3.0 ± 0.8	0.028	0.131	0.999	0.059	0.999	0.082	0.999
ΔT _i (ms)	–75 ± 42	–46 ± 33	–58 ± 35	–49 ± 30	0.253	–	–	–	–	–	–
ΔT _e (ms)	–273 ± 133	–250 ± 116	–261 ± 97	–281 ± 103	0.961	–	–	–	–	–	–
ΔVO ₂ (ml/min/100 g)	–1.4 ± 0.8	–1.9 ± 1	–1.5 ± 1.1	–1.5 ± 0.9	0.69	–	–	–	–	–	–
ΔVCO ₂ (ml/min/100 g)	–0.2 ± 0.4	–0.3 ± 0.5	–0.2 ± 0.6	–0.2 ± 0.5	0.886	–	–	–	–	–	–
ΔV _E /VCO ₂	59 ± 30	35 ± 31	36 ± 18	38 ± 18	0.115	–	–	–	–	–	–

f_R, respiratory frequency (brpm, breaths per min); V_E, minute ventilation; V_T, tidal volume; V_T/T_i, mean inspiratory flow; T_i, inspiratory time; T_e, expiratory time; SD1, short-term respiratory timing variability; SD2, long-term respiratory timing variability; VO₂, oxygen consumption; VCO₂, carbon dioxide production; V_E/VCO₂, ventilatory equivalent; VEH, autoclaved deionised water; ABX, antibiotic-administration; VEH-FMT, VEH followed by faecal microbiota transfer; ABX-FMT, antibiotic administration followed by faecal microbiota transfer. Data are shown as mean ± SD and were statistically compared using one-way ANOVA with Bonferroni *post hoc* where appropriate, or non-parametric Kruskal-Wallis test with Dunn's *post hoc*, where appropriate. Each *p*-value is adjusted to account for multiple comparisons. *p*-values shown in bold highlight significant differences. Responses are expressed as absolute change from baseline (Δ parameter).

Table 6
Respiratory timing variability, apnoeas and sighs during hypercapnia in behaving rats during quiet rest.

	VEH (n = 10)	ABX (n = 10)	VEH-FMT (n = 10)	ABX-FMT (n = 10)	One-way ANOVA	VEH vs ABX	VEH-FMT vs ABX-FMT	VEH vs VEH-FMT	ABX vs ABX-FMT	VEH vs ABX-FMT	ABX vs VEH-FMT
T _i SD1 (ms)	24 ± 6	18 ± 8	17 ± 5	17 ± 4	0.042	0.232	0.999	0.091	0.999	0.083	0.999
T _i SD2 (ms)	55 ± 27	29 ± 14	30 ± 11	36 ± 10	0.004	0.006	0.999	0.019	0.701	0.511	0.999
T _e SD1 (ms)	28 ± 46	54 ± 27	53 ± 29	51 ± 22	0.697	–	–	–	–	–	–
T _e SD2 (ms)	109 ± 55	73 ± 32	78 ± 34	76 ± 28	0.329	–	–	–	–	–	–
T _{tot} SD1 (ms)	80 ± 29	64 ± 31	62 ± 26	61 ± 24	0.375	–	–	–	–	–	–
T _{tot} SD2 (ms)	161 ± 88	108 ± 51	103 ± 36	94 ± 41	0.170	–	–	–	–	–	–
Apnoea index (events/h)	5.5 ± 5.5	9.5 ± 5.5	11.0 ± 6.1	12.0 ± 8.6	0.159	–	–	–	–	–	–
Apnoea duration (s)	2.3 ± 1.0	2.5 ± 0.8	2.2 ± 0.5	2.2 ± 0.7	0.689	–	–	–	–	–	–
Sigh frequency (events/h)	14 ± 6	14 ± 5	15 ± 7	19 ± 11	0.87	–	–	–	–	–	–

T_i, inspiratory time; T_e, expiratory time; T_{tot}, total breath duration; SD1, short-term respiratory timing variability; SD2, long-term respiratory timing variability; VEH, autoclaved deionised water; ABX, antibiotic-treated; VEH-FMT, VEH followed by faecal microbiota transfer; ABX-FMT, antibiotic-treated followed by faecal microbiota transfer. Data are shown as mean ± SD and were statistically compared using one-way ANOVA with Bonferroni *post hoc* where appropriate, or non-parametric Kruskal-Wallis test with Dunn's *post hoc*, where appropriate. Each *p*-value is adjusted to account for multiple comparisons. *p*-values shown in bold highlight significant differences.

however allogenic FMT had transient benefits on insulin sensitivity which was driven by baseline faecal microbiota composition [62].

Caecum weights of ABX-FMT rats were lighter than that of ABX rats, but did not recover completely to VEH values. After discontinuing antibiotic exposure, gastrointestinal responses of ABX-FMT rats, assessed qualitatively by faecal output, returned to levels equivalent to VEH rats. Similar results were observed both in rodent and clinical studies where FMT was used to treat *Clostridium difficile* infection and sepsis [58,63]. Thus, ABX-induced alterations to the microbiota were not reversed by FMT intervention in our study. Indeed, FMT itself led to significant modification of the microbiota, establishing a separate model of microbiota disruption in our study (VEH-FMT and ABX-FMT groups), with distinct microbiota signatures compared with that of VEH animals.

4.2. Chronic antibiotic administration and faecal microbiota transfer blunt ventilatory responses to hypoxia and hypercapnia

To date few studies have examined the consequences of manipulation of the gut microbiota on the control of breathing. We

previously revealed enhanced variability of breathing frequency during normoxic breathing, and altered ventilation during hypoxic and hypercapnic chemostimulation in adult rats exposed to antecedent pre-natal stress [15]. Significant correlations were found between respiratory frequency during hypercapnia and bacterial genera of the Firmicutes phylum [15], suggesting a potential influence of alterations in the gut microbiota on the control of respiratory rhythm during CO₂ exposure.

We reasoned that perturbation of the gut microbiota by ABX would elicit a distinctive respiratory control signature. In conscious behaving rats during quiet rest, no apparent aberrant respiratory control phenotype was evident in ABX rats during normoxia such that we observed normal values for ventilation and metabolism equivalent to VEH. Moreover, VEH-FMT and ABX-FMT rats were similar to VEH revealing the remarkable capacity of the neural network to maintain homeostasis in the light of major disruption to brainstem monoamine concentrations (discussed below). V_E/VCO₂ was decreased in VEH-FMT rats compared with VEH during normoxia, revealing a relatively depressed level of ventilation *per se* in VEH-FMT rats.

Table 7
Baseline ventilation, blood gases and cardiovascular measurements in anaesthetised rats.

	VEH (n = 8–10)	ABX (n = 8)	VEH-FMT (n = 9)	ABX-FMT (n = 10)	One-way ANOVA	VEH vs ABX	VEH-FMT vs ABX-FMT	VEH vs VEH-FMT	ABX vs ABX-FMT	VEH vs ABX-FMT	ABX vs VEH-FMT
f _R (brpm)	99 ± 13	103 ± 9	92 ± 14	88 ± 12	0.066	–	–	–	–	–	–
V _E (ml/min/100 g)	35.9 ± 3.7	36.3 ± 4.6	31.6 ± 6.7	30.2 ± 12	0.071	–	–	–	–	–	–
V _T (ml/100 g)	0.36 ± 0.03	0.35 ± 0.04	0.34 ± 0.05	0.38 ± 0.06	0.312	–	–	–	–	–	–
ETCO ₂	5.9 ± 0.6	5.9 ± 0.9	5.6 ± 0.6	5.6 ± 0.6	0.536	–	–	–	–	–	–
pH	7.34 ± 0.02	7.36 ± 0.06	7.36 ± 0.03	7.37 ± 0.03	0.272	–	–	–	–	–	–
PaCO ₂ (mmHg)	48.2 ± 3.9	47.2 ± 7.9	48.6 ± 5.2	45.2 ± 4.3	0.272	–	–	–	–	–	–
PaO ₂ (mmHg)	107 ± 16	100 ± 8	106 ± 10	104 ± 6	0.712	–	–	–	–	–	–
[HCO ₃ ⁻] (mmol/l)	26.3 ± 1.2	26.4 ± 2.0	27.1 ± 1.4	26.1 ± 0.9	0.106	–	–	–	–	–	–
TCO ₂ (mmol/l)	27.7 ± 1.3	27.8 ± 2.4	28.3 ± 1.5	27.5 ± 1.0	0.303	–	–	–	–	–	–
S _a O ₂ (%)	97.5 ± 1.1	97.3 ± 0.9	97.7 ± 0.7	97.6 ± 0.7	0.987	–	–	–	–	–	–
[Na ⁺] (mmol/l)	136.6 ± 2.6	137.0 ± 1.8	135.4 ± 1.4	135.1 ± 1.4	0.078	–	–	–	–	–	–
[K ⁺] (mmol/l)	4.2 ± 0.1	4.0 ± 0.2	4.2 ± 0.1	4.2 ± 0.2	0.149	–	–	–	–	–	–
Haematocrit (%)	51.7 ± 2.9	47.9 ± 2.0	48.3 ± 2.9	49.7 ± 2.3	0.016	0.024	0.999	0.062	0.665	0.792	0.999
[Hb] (g/dl)	17.5 ± 0.9	16.3 ± 0.7	16.1 ± 1.4	16.1 ± 2.9	0.021	0.028	0.999	0.082	0.999	0.596	0.999
MAP (mmHg)	96 ± 9	93 ± 12	90 ± 10	94 ± 13	0.712	–	–	–	–	–	–
DBP (mmHg)	73 ± 9	74 ± 13	66 ± 7	70 ± 12	0.463	–	–	–	–	–	–
SBP (mmHg)	148 ± 15	119 ± 12	140 ± 15	147 ± 15	0.0005	0.0007	0.999	0.999	0.001	0.999	0.024
HR (bpm)	410 ± 29	407 ± 40	389 ± 27	410 ± 28	0.438	–	–	–	–	–	–

f_R, respiratory frequency (brpm, breaths per min); V_E, minute ventilation; V_T, tidal volume; ETCO₂, end-tidal carbon dioxide production; PaCO₂, partial pressure of arterial carbon dioxide; PaO₂, partial pressure of arterial oxygen; [HCO₃⁻], bicarbonate concentration; TCO₂, total carbon dioxide; S_aO₂, arterial oxygen saturation; [Na⁺], sodium concentration; [K⁺], potassium concentration; [Hb], haemoglobin concentration; MAP, mean arterial blood pressure; SBP, systolic blood pressure; DBP, diastolic blood pressure; HR, heart rate (bpm, beat per min); dP/dt max, maximum left ventricular contractility; PP, pulse pressure; VEH, autoclaved deionised water; ABX, antibiotic-treated; VEH-FMT, VEH followed by faecal microbiota transfer; ABX-FMT, antibiotic-treated followed by faecal microbiota transfer. Data are shown as mean ± SD and were statistically compared using one-way ANOVA with Bonferroni *post hoc* where appropriate, or non-parametric Kruskal-Wallis test with Dunn's *post hoc*, where appropriate. Each *p*-value is adjusted to account for multiple comparisons. *p*-values shown in bold highlight significant differences.

Compared with VEH, ABX depressed the peak hypoxic ventilatory response and respiratory frequency component of the response during the first 2 min of exposure to hypoxia. A similar blunted minute ventilation and frequency response was observed in VEH-FMT rats compared with VEH revealing a consistent outcome in response to manipulation of the gut microbiota. Interestingly, respiratory timing variability was unaffected by ABX or FMT. Moreover, analysis of steady-state responses during the last 5 min of hypoxic exposure revealed that there was no aberrant respiratory phenotype evident in ABX or FMT rats. Our findings in ABX and FMT rats of a blunted minute ventilation and respiratory frequency response in phase 1 of the hypoxic ventilatory response is similar to the depressed hypoxic ventilatory response evident in adult rats exposed to pre-natal stress, where a significantly depressed respiratory frequency response to hypoxia was also observed [15]. It is plausible that manipulation of the gut microbiota resulted in altered integration of chemosensory inputs from the carotid bodies (the primary peripheral oxygen sensors) at the level of the nucleus tractus solitarius, leading to the development of a blunted frequency response to hypoxia. It is intriguing to consider that microbiota disruption may have resulted in re-programming of the carotid bodies, resulting in modified chemosensory afferent discharge to the brain, but this remains to be tested in future work. Although the peak hypoxic ventilatory response was blunted, the steady-state response (phase 2) was intact, again highlighting the robust capacity of the chemoreflex pathway in maintaining respiratory homeostasis in our models.

Chemoactivation of ventilation in response to hypercapnic stress (elevated inspired CO_2) revealed a robust blunted V_E response to CO_2 challenge in ABX rats compared with VEH, a ventilatory depression manifest as a reduced f_R response to hypercapnia (bradypnoea), which was maintained throughout the hypercapnic challenge. Manipulation of the gut microbiota had no effect on metabolic responses (VCO_2) to hypercapnia. Thus, the ventilatory equivalent for carbon dioxide (V_E/VCO_2), which relates ventilation to the prevailing metabolism, was depressed in ABX rats compared with VEH rats, highlighting inadequate ventilation to meet metabolic demand (hypoventilation). Microbiota disruption by FMT resulted in decreased ventilation in hypercapnia in FMT groups to levels similar to that seen in ABX animals, and significantly below that of VEH rats. Therefore, two modes of disrupted microbiota in our study were associated with depressed ventilatory response to hypercapnia. Respiratory timing variability and associated respiratory behaviours such as apnoeas and sighs were essentially unaffected by microbiota manipulation.

The disruptions to ventilation in response to hypoxic or hypercapnic stress observed in behaving animals using whole-body plethysmography, were not evident in urethane-anaesthetised animals, suggesting that the changes in respiratory control may be state-dependent [64]. Indeed anaesthesia depresses respiratory drive and chemoresponsiveness [65], and this may have masked the otherwise blunted ventilatory responsiveness to hypercapnic stress and the blunted peak ventilatory response to hypoxia in animals with manipulations to the microbiota. Alternatively, it may be that chemoreflex-driven homeostatic control of breathing is unaffected in ABX and FMT rats, but that the composite behavioural response to hypoxic and hypercapnic stress—manifest in the integrated respiratory behavioural response to challenges—is blunted.

The hypercapnic stimulus used in our study was modest, sufficient to evoke a ventilatory response through the activation of central nervous system CO_2 chemoreceptors, but not intended as an overt behavioural stressor. Nevertheless, hypercapnia can provoke fear-associated responses and there are strong links between emotion and respiratory behaviour. Indeed, ventilatory hypersensitivity to CO_2 is a hallmark of panic disorder in susceptible individuals. Thus, it is possible in our study that manipulation of the microbiota altered neurochemistry in brain regions such as the amygdala [36], which is known to modulate ventilatory responsiveness to CO_2 [66]. Dopamine is a candidate neurotransmitter in emotion-associated respiratory control, with evidence

that breathing is modulated by dopaminergic signalling in the basolateral amygdala [67]. The data from behaving rats demonstrate a capacity for aberrant respiratory plasticity in animals with altered gut microbiota, supporting the concept that the microbiota-gut-brainstem axis may function as an important modulator of the respiratory control network, either directly or indirectly. Blunted CO_2 chemoreflex ventilatory responses are physiologically significant as they increase the risk of the development of systemic acidosis in circumstances of elevated CO_2 (e.g. sleep, pulmonary and respiratory control diseases, respiratory depression by drugs) [68,69]. Hypercapnic acidosis can compromise the function of neural networks and systemic tissues due to pH imbalance. As such, disruptions to the microbiota could *via* aberrant respiratory control, exert deleterious effects on whole body homeostasis.

4.3. Chronic antibiotic administration decreases systolic blood pressure

Cardiovascular control is complex and multifaceted with recent studies in animal models and humans demonstrating the contribution of the gut microbiome to the regulation of blood pressure [14,34,35]. In spontaneously hypertensive rat and angiotensin-II hypertensive rat models, shifts in microbiota richness and increases in the Firmicutes: Bacteroidetes ratio are evident [35]. Of note, FMT from hypertensive human donors to germ-free mice elevates blood pressure in the recipient mice, which was observed to be transferrable through the microbiota [34]. Similarly, it has been demonstrated that antibiotic-treated normotensive rats that received a FMT of donor faeces from hypertensive rats subsequently developed hypertension [14]. Bacterial metabolites are associated with the development of high blood pressure; specifically, a decrease in butyrate-producing and acetate-producing bacteria, which promote intestinal barrier integrity, and an increase in lactate-producing bacteria are each associated with hypertension [12,14,35]. Oral administration of a probiotic (*Clostridium butyricum*) or a prebiotic (Hylon VII) prevented microbiota disruption, increased acetate levels and prevented the development of hypertension in a rat model of obstructive sleep apnoea [17]. Additionally, caecal acetate administration prevented obstructive sleep apnoea induced hypertension [17]. The anti-inflammatory antibiotic minocycline was shown to ameliorate hypertension and reduce the Firmicutes:Bacteroidetes ratio in an angiotensin II hypertensive rat model [35]. The absence of gut microbiota in germ free mice appears to be protective against angiotensin II induced hypertension and vascular dysfunction [70]. Our study revealed that chronic broad-spectrum ABX intervention results in lower systolic blood pressure and pulse pressure, although no difference was evident in mean arterial blood pressure.

Evidence is accruing in support of a microbial influence over cardiovascular control although a defined microbiota signature essential to the maintenance of normal blood pressure has yet to be determined. An enrichment in *Lactobacillus*, *Bifidobacterium* and *Allobaculum* along with a reduction in *Lachnospiraceae*, *Lactococcus*, *Blautia*, *Coprobacillus* and *Erysipelotrichaceae* species occurred in a rat model of obstructive sleep apnoea compared with sham. In sham animals, prebiotic (Hylon VII) treatment increased the abundance of acetate-producing genera, including *Blautia*, *Colinsella*, *Bifidobacterium* and *Ruminococcus*, preventing the development of hypertension [17]. Intriguingly, a dramatic proliferation of certain genera such as *Prevotella* and *Klebsiella* has been shown both in pre-hypertensive and hypertensive individuals compared with normotensive controls. In this clinical population, Firmicutes including *Oscillibacter*, *Roseburia* and *Blautia*, *Bifidobacterium* from Actinobacteria phylum and *Akkermansia* from Verrucomicrobiaceae phylum were 5 out of 11 genera enriched in healthy normotensive controls compared with pre-hypertensive and hypertensive individuals [34]. Indeed, these genera were in the top 45% of highly abundant genera in VEH, VEH-FMT and ABX-FMT groups. Genera which were highly abundant in pre-hypertensive and hypertensive humans were not abundant in this study, but comparisons between species may not be appropriate. Of interest, *Blautia* and *Bifidobacterium*

were highly abundant in prebiotic-treated normotensive rodents and healthy normotensive controls [17,34]. These acetate-producing bacterial taxa may have a role in the regulation of normal blood pressure [15]. Correlation analysis in our study revealed no associations between genera and blood pressure parameters. However, *Anaerovorax*, of Firmicutes phylum positively correlated with basal heart rate.

4.4. Cardiorespiratory responsiveness to vagal afferent nerve stimulation is unaffected by chronic antibiotic administration and faecal microbiota transfer

The afferent vagal pathway provides crucial signalling between the gut microbiota and the central nervous system [71]. Alterations in gut microbiota composition or diversity, resulting in differential production of bacterial metabolites, have been shown to influence afferent vagal traffic [20,72]. Vagal afferents innervate the nucleus tractus solitarius, a critical relay hub in the integration of cardiorespiratory control [73]. The 5-HT₃ receptor agonist, PBG, stimulates pulmonary vagal afferent C-fibres manifesting the classical chemoreflex characterised by apnoea and post-apnoea tachypnoea, bradycardia and a fall in blood pressure [43,44]. Manipulation of the gut microbiota could conceivably manifest abnormal vagal afferent signalling and aberrant central processing of sensory inputs. However, in our study, there was no difference in the cardiorespiratory efferent responses to PBG challenge. We conclude that manipulation of the microbiota by ABX and FMT interventions does not alter the cardiorespiratory response to the vagal afferent pulmonary C-fibre stimulation, notwithstanding evidence of significant disruptions in brainstem monoamine concentrations. Whereas PBG can also induce neurotransmitter release centrally in the nucleus accumbens [74] and the nucleus tractus solitarius [75], we confirmed in our study that cardiorespiratory effects were mediated exclusively by vagal afferent feedback since responses were abolished following bilateral cervical vagotomy. Examination of vagal afferent activation from other peripheral sites, notably the gut, was not performed in this study, but would be interesting to determine in future work.

4.5. Chronic antibiotic administration and faecal microbiota transfer alter brainstem monoamine and monoamine metabolite concentrations

We examined the concentrations of brainstem monoamines important in the neuromodulation of cardiorespiratory control with a particular interest in monoamines and metabolites that play a role in central chemoreception. Significant disruptions to monoamine, monoamine precursor and metabolite concentrations were determined in the brainstem of ABX and FMT rats, an outcome that coincides with depressed hypercapnic ventilation.

Noradrenaline is a potent modulator of breathing [76,77]. We found no change in brainstem noradrenaline concentration between groups. 5-HT is a pivotal neuromodulator of the respiratory motor network and primarily has an excitatory effect on breathing [78]. It is well established that pharmacological manipulation of serotonergic signalling affects respiratory motor output [79,80]. Transgenic mice lacking central 5-HT neurons show a significant reduction in the hypercapnic ventilatory response [81–83] and lesions of raphé serotonergic neurons decrease the respiratory response to hypercapnia [84]. Pharmacological manipulation of 5-HT affects ventilation and arousal during hypercapnia [85,86]. Our data revealed a blunted ventilatory response to hypercapnia in ABX rats. However, 5-HT concentrations were not changed in ABX rats, thus, it is not likely that 5-HT is implicated in the depressed ventilatory responsiveness observed in ABX rats. 5-HT concentrations were significantly increased in ABX-FMT compared with VEH with no change evident in VEH-FMT rats. This suggests that changes in brainstem 5-HT were not pivotal to hypercapnic ventilatory depression. Interestingly, an increase in 5-HT turnover was observed in the hippocampus and pre-frontal cortex following ABX treatment in rats [36], germ free mice [87] and acutely stressed mice [37].

Dopamine significantly contributes to the central control of breathing [88]. Transgenic mice lacking dopaminergic neurons or dopamine transport proteins exhibit severe breathing disturbances such as hypoventilation, apnoea and altered hypoxic ventilatory response [89,90]. Similarly, blunted respiratory frequency during hypercapnic breathing was observed in rat models of Parkinson's disease with confirmed degeneration of tyrosine hydroxylase expressing neurons in the substantia nigra and a reduction in chemosensitive neurons (Phox2b-expressing and fos-activated) in the retrotrapezoid nucleus [91,92], a key brainstem site for CO₂ chemosensitivity [93]. The modulatory influence of dopamine on respiratory physiology is complex and depends on target receptor sub-families [94]. There are 2 classes of dopamine receptors, D₁-like (D₁ and D₅) and D₂-like (D₂, D₃ and D₄) receptors [95], with D₁, D₂ and D₄ receptors having a significant neuromodulatory role in respiration [88,96,97]. Dopaminergic neurons within the brainstem reinforce CO₂-dependent respiratory drive and increase minute ventilation, predominantly through the D₁ receptor [97,98]. Thus, it appears that D₁ receptor activation increases respiratory neuron excitability, whereas D₂ and D₄ receptor stimulation depresses respiratory rhythm [96,97,99]. Our data reveal an increase in brainstem dopamine turnover in ABX rats and depressed ventilation during hypercapnia compared with VEH rats. Similar findings are reported in Parkinson's disease models [91,92,100]. An increase in the dopamine metabolite HVA was also evident in the cerebellum of ABX rats compared with VEH rats in our study (Supplementary Table 10). Increased concentrations of HVA were observed in the prefrontal cortex and amygdala of ABX-treated rodents [36,37]. We observed depressed respiratory frequency responses to hypercapnic stress in ABX and FMT groups, which may have related to increased dopaminergic signalling via D₂ and D₄ receptors [96,97,99].

Our findings demonstrate that disruption to the gut microbiota results in altered neurochemistry at the level of the brainstem and cerebellum, with striking effects on dopamine concentrations and dopamine turnover. Correlation analysis revealed significant associations between brainstem neurochemistry and genera from 6 phyla, suggesting a potential link. Of particular interest correlations were found between L-DOPA, DA, HVA and HVA/DA and genera predominantly of Firmicutes phylum; *Ruminococcaceae* UCG-005, *Peptoclostridium*, *Bacillus*, *Erysipelotrichaceae* UCG-004, *Ruminococcaceae* UCG-011, *Lachnospirillum* 10, *Clostridiales* vadinBB60 group uncultured bacterium and *Ruminococcaceae* UCG-009. Brainstem monoamines and metabolites also correlate with *Coriobacteriaceae* uncultured (Actinobacteria) *Bacteroidetes* VC2.1 Bac22 uncultured (Bacteroidetes), *Gastranaerophilales* uncultured organism (Cyanobacteria), *Helicobacter* (Proteobacteria) and *Mucispirillum* (Deferribacteres). We acknowledge that correlations were often weak and in any event do not provide evidence of a mechanistic link. Disrupted brainstem neurochemistry is also evident in other models of microbiota perturbation. Germ free mice have increased 5-HT in hippocampal regions and acutely stressed and non-stressed ABX-treated animals have an increase in HVA in prefrontal cortex and amygdala [36,37,87]. To assess if altered afferent vagal nerve communication (gut-brain axis) contributed to the altered brainstem neurochemistry and respiratory behaviour, future studies exploring manipulation of the gut microbiota in vagotomised animals are required. However, vagal axotomy may itself evoke plasticity with the brainstem neural circuits controlling cardiorespiratory control, which may be a confounding factor in such studies.

4.6. Chronic antibiotic administration and faecal microbiota transfer increase distal ileum permeability

Altered intestinal permeability has been described in various models of disrupted microbiota including a mouse model of autism [7], spontaneously hypertensive rat [13], and rat models of maternal separation stress [15,101] and pre-natal stress [15]. The dysfunctional barrier of the distal ileum in ABX and FMT rats in our study is consistent with

reports of disrupted intestinal permeability in response to specific antibiotics, which also perturb the microbiota [102,103]. An impaired epithelial barrier can induce low-grade inflammation and facilitate the passage of bacterial constituents, such as lipopolysaccharide across the epithelium into systemic tissues [104]. It is conceivable that the 'leaky' distal ileum could have, at least partially, contributed to modulation of brainstem neurochemistry and depressed ventilatory responsiveness to CO₂. However, ABX rats may have limited maladies associated with intestinal barrier breach due to reduced bacterial components and/or the direct effects of antibiotics on other inflammatory mediators.

The shifts evident in *Helicobacter* and *Mucispirillum* genera are of particular interest with respect to gastrointestinal health. Of critical importance, the highest log-fold change occurred in *Helicobacter*, which was significantly increased both in VEH-FMT and ABX-FMT rats compared with VEH rats. Guo et al. 2009 found that *Helicobacter pylori* was increased in the stomach of Balb/c mice in response to stress [105]. A similar stress could have been evoked by the use of oral gavage, resulting in increased abundance of *Helicobacter*. The dominance of various species from *Helicobacter* genera in the gut microbiota coincides with gastrointestinal disorders in humans and rodents, often triggering intestinal inflammatory pathogenesis [106]. A mucin degrading bacterium *Mucispirillum* was decreased in VEH-FMT and ABX-FMT rats compared with VEH. Increased abundance of *Mucispirillum* coincides with inflammatory response in germ-free mice [107], in a model of colitis [108], and in age-related inflammation in rodents [109]. It is plausible that *Helicobacter* proliferated at the expense of *Mucispirillum*. Intestinal pathogenesis could have occurred as a result of insults to the microbiota associated with our interventions.

4.7. Limitations

Our FMT strategy was designed to replenish the microbiota of ABX rats. To control for the FMT intervention, VEH rats also received FMT and were studied in parallel. However, FMT *per se* caused major disruption to the microbiota composition and diversity compared with VEH rats. As such, our study did not allow us to determine if restoration of normal (control) gut microbiota was associated with restoration of normal (control) brainstem neurochemistry and ventilatory responsiveness to hypercapnia. Whereas this is a limitation of the study, it nevertheless provided unexpected additional test groups (FMT groups), wherein gut microbiota disruptions were shown to be related to altered brainstem neurochemistry and blunted ventilatory responsiveness to CO₂, in essence confirming the observations made in ABX rats compared with VEH rats. Future studies could explore the capacity to transfer the phenotypes described in the present study from ABX donor to naïve recipient animals. Moreover, it would be interesting to explore FMT strategies designed to recover brainstem neurochemistry and ventilatory responsiveness to hypercapnia in ABX-treated rats.

DNA concentrations in caecal samples from ABX rats were critically low, likely a result of the broad-spectrum antibiotic cocktail depleting bacteria and thus detectable bacterial DNA. This prevented the analysis of microbiota composition and diversity analysis as 16S rRNA sequencing was not possible in this group. Thus, correlation analysis was performed with metadata and microbiota composition from three groups (VEH, VEH-FMT and ABX-FMT).

Our study design was such that we were unable to perform correlations between breathing parameters and microbiota in ABX-treated rats, since ABX rats studied in the plethysmograph proceeded to FMT intervention.

4.8. Summary and conclusions

Using two modes to manipulate the gut microbiota (ABX and FMT), our study suggests that perturbation to the gut microbiota has consequences for brainstem neurochemistry and respiratory control. Our study reveals the capacity for chronic antibiotic administration and

faecal microbiota transfer to affect respiratory behaviour, blunting a critical homeostatic reflex defence or integrated behavioural response to acute hypercapnic stress, with resultant consequences for acid-base status. Our results may have relevance to human respiratory disorders of the lungs or neural control networks, such as chronic obstructive pulmonary diseases and sleep disordered breathing, where there is evidence of altered gut microbiota composition. Blunted chemoreflex control of breathing, wherein arterial blood CO₂ levels can rise due to inadequate ventilatory drive, is a risk for the development of significant respiratory acidosis, with whole-body consequences. Our study adds to emerging evidence providing a rationale for manipulation of the gut microbiota as an adjunctive therapy in cardiorespiratory diseases.

Supplementary data to this article can be found online at <https://doi.org/10.1016/j.ebiom.2019.03.029>.

Competing interests

JFC is in receipt of research funding from 4D-Pharma, Mead Johnson, Nutricia, Dupont and Cremo and has been an invited speaker at meetings organised by Mead Johnson, Alkermes, Abbott Nutrition, Danone Nutricia and Janssen. All other authors report no financial, professional or personal conflicts of interest relating to this publication.

Authors' contributions

KMO'C: experimental design; acquisition of data; data and statistical analysis and interpretation of data; drafting of the original manuscript; EFL: *in vivo* studies: experimental design; acquisition of data; interpretation of data; drafting of the original manuscript; KMO'C and EFL contributed equally to the study; AVG: Ussing chamber studies: experimental design; acquisition of data; statistical analysis; interpretation of data; CRS; 16S rRNA sequencing: acquisition of data; data and statistical analysis; FF: 16S rRNA sequencing: acquisition of data; MCC: DNA extraction; PD: data and statistical analysis; DPB: experimental design; data analysis; TB: correlation analysis: interpretation of data; CS: critical revision of the manuscript for important intellectual content; GC: HPLC studies: interpretation of data; critical revision of the manuscript for important intellectual content; JFC: experimental design; critical revision of the manuscript for important intellectual content; KDO'H: experimental design; interpretation of physiological data; drafting and critical revision of the manuscript for important intellectual content.

Funding

This project was funded by the Department of Physiology, and the APC Microbiome Ireland (funded by Science Foundation Ireland (SFI/12/RC/2273)), University College Cork, Ireland. The institution had no role in the study design, data collection, data analysis, interpretation or writing of the manuscript.

Acknowledgments

The authors wish to acknowledge the technical expertise of Dr. Paul Cotter, Dr. Fiona Crispie and Dr. Laura Finnegan from the Teagasc Sequencing Facility at Moorepark and we thank them for their assistance with MiSeq sequencing. The authors are grateful to staff of the Biological Services Unit, University College Cork for their support with animal housing and welfare. We are grateful to Prof. Thomas Walther, Department of Pharmacology & Therapeutics, University College Cork for the use of equipment to measure cardiac contractility.

References

- [1] Dinan TG, Cryan JF. The microbiome-gut-brain axis in health and disease. *Gastroenterol Clin N Am* 2017;46(1):77–89.
- [2] Bordenstein SR, Theis KR. Host biology in light of the microbiome: ten principles of Holobionts and Hologenomes. *PLoS Biol* 2015;13(8):e1002226.

- [3] Sudo N, Chida Y, Aiba Y, Sonoda J, Oyama N, Yu XN, et al. Postnatal microbial colonization programs the hypothalamic-pituitary-adrenal system for stress response in mice. *J Physiol* 2004;558:263–75 Pt 1.
- [4] O'Mahony SM, Felice VD, Nally K, Savignac HM, Claesson MJ, Scully P, et al. Disturbance of the gut microbiota in early-life selectively affects visceral pain in adulthood without impacting cognitive or anxiety-related behaviors in male rats. *Neuroscience* 2014;277:885–901.
- [5] Kelly JR, Borre Y, C OB, Patterson E, El Aidi S, Deane J, et al. Transferring the blues: depression-associated gut microbiota induces neurobehavioural changes in the rat. *J Psychiatr Res* 2016;82:109–18.
- [6] Burokas A, Arbolea S, Moloney RD, Peterson VL, Murphy K, Clarke G, et al. Targeting the microbiota-gut-brain Axis: prebiotics have anxiolytic and antidepressant-like effects and reverse the impact of chronic stress in mice. *Biol Psychiatry* 2017;82(7):472–87.
- [7] Golubeva AV, Joyce SA, Moloney G, Burokas A, Sherwin E, Arbolea S, et al. Microbiota-related changes in Bile Acid & Tryptophan Metabolism are associated with gastrointestinal dysfunction in a mouse model of autism. *EBioMedicine* 2017;24:166–78.
- [8] Stilling RM, Moloney GM, Ryan FJ, Hoban AE, Bastiaanssen TF, Shanahan F, et al. Social interaction-induced activation of RNA splicing in the amygdala of microbiome-deficient mice. *eLife* 2018;7.
- [9] De Palma G, Blennerhassett P, Lu J, Deng Y, Park AJ, Green W, et al. Microbiota and host determinants of behavioural phenotype in maternally separated mice. *Nat Commun* 2015;6:7735.
- [10] Neufeld KM, Kang N, Bienenstock J, Foster JA. Reduced anxiety-like behavior and central neurochemical change in germ-free mice. *Neurogastroenterol Motil* 2011;23(3) [255–64, e119].
- [11] Burokas A, Moloney RD, Dinan TG, Cryan JF. Microbiota regulation of the mammalian gut-brain axis. *Adv Appl Microbiol* 2015;91:1–62.
- [12] Durgan DJ, Ganesh BP, Cope JL, Ajami NJ, Phillips SC, Petrosino JF, et al. Role of the gut microbiome in obstructive sleep Apnea-induced hypertension. *Hypertension* 2016;67(2):469–74.
- [13] Santisteban MM, Qi Y, Zubcevic J, Kim S, Yang T, Shenoy V, et al. Hypertension-linked pathophysiological alterations in the gut. *Circ Res* 2017;120(2):312–23.
- [14] Adnan S, Nelson JW, Ajami NJ, Venna VR, Petrosino JF, Bryan Jr RM, et al. Alterations in the gut microbiota can elicit hypertension in rats. *Physiol Genomics* 2017;49(2):96–104.
- [15] Golubeva AV, Crampton S, Desbonnet L, Edge D, O'Sullivan O, Lomasney KW, et al. Prenatal stress-induced alterations in major physiological systems correlate with gut microbiota composition in adulthood. *Psychoneuroendocrinology* 2015;60:58–74.
- [16] Lucking EF, O'Connor KM, Strain CR, Fouhy F, Bastiaanssen TFS, Burns DP, et al. Chronic intermittent hypoxia disrupts cardiorespiratory homeostasis and gut microbiota composition in adult male Guinea-pigs. *EBioMedicine* 2018;38:191–205.
- [17] Ganesh BP, Nelson JW, Eskew JR, Ganesan A, Ajami NJ, Petrosino JF, et al. Prebiotics, probiotics, and acetate supplementation prevent hypertension in a model of obstructive sleep Apnea. *Hypertension Dallas Tex: 1979* 2018;72(5):1141–50.
- [18] Garcia III AJ, Zanella S, Koch H, Doi A, Ramirez JM. Chapter 3—networks within networks: the neuronal control of breathing. *Prog Brain Res* 2011;188:31–50.
- [19] Alheid GF, McCrimmon DR. The chemical neuroanatomy of breathing. *Respir Physiol Neurobiol* 2008;164(1–2):3–11.
- [20] Bonaz B, Bazin T, Pellissier S. The Vagus nerve at the interface of the microbiota-gut-brain Axis. *Front Neurosci* 2018;12:49.
- [21] Fuller DD, Mitchell GS. Respiratory neuroplasticity - overview, significance and future directions. *Exp Neurol* 2017;287(Pt 2):144–52.
- [22] Almado CE, Machado BH, Leao RM. Chronic intermittent hypoxia depresses afferent neurotransmission in NTS neurons by a reduction in the number of active synapses. *J Neurosci* 2012;32(47):16736–46.
- [23] Kumar P, Prabhakar NR. Peripheral chemoreceptors: function and plasticity of the carotid body. *Compr Physiol* 2012;2(1):141–219.
- [24] Hocker AD, Stokes JA, Powell FL, Huxtable AG. The impact of inflammation on respiratory plasticity. *Exp Neurol* 2017;287(Pt 2):243–53.
- [25] Peng YJ, Nanduri J, Yuan G, Wang N, Deneris E, Pendyala S, et al. NADPH oxidase is required for the sensory plasticity of the carotid body by chronic intermittent hypoxia. *J Neurosci* 2009;29(15):4903–10.
- [26] Soliz J, Tam R, Kinkead R. Neonatal maternal separation augments carotid body response to hypoxia in adult males but not female rats. *Front Physiol* 2016;7:432.
- [27] Fournier S, Steele S, Julien C, Gulemetova R, Caravagna C, Soliz J, et al. Gestational stress promotes pathological apneas and sex-specific disruption of respiratory control development in newborn rat. *J Neurosci* 2013;33(2):563–73.
- [28] Gulemetova R, Kinkead R. Neonatal stress increases respiratory instability in rat pups. *Respir Physiol Neurobiol* 2011;176(3):103–9.
- [29] Kinkead R, Guertin PA, Gulemetova R. Sex, stress and their influence on respiratory regulation. *Curr Pharm Des* 2013;19(24):4471–84.
- [30] Bavis RW. Developmental plasticity of the hypoxic ventilatory response after perinatal hyperoxia and hypoxia. *Respir Physiol Neurobiol* 2005;149(1–3):287–99.
- [31] Tripathi A, Melnik AV, Xue J, Poulsen O, Meehan MJ, Humphrey G, et al. Intermittent hypoxia and hypercapnia, a hallmark of obstructive sleep Apnea, alters the gut microbiome and metabolome. *mSystems* 2018;3(3).
- [32] Moreno-Indias I, Torres M, Montserrat JM, Sanchez-Alcoholado L, Cardona F, Tinahones FJ, et al. Intermittent hypoxia alters gut microbiota diversity in a mouse model of sleep apnoea. *Eur Respir J* 2015;45(4):1055–65.
- [33] Moreno-Indias I, Torres M, Sanchez-Alcoholado L, Cardona F, Almendros I, Gozal D, et al. Normoxic recovery mimicking treatment of sleep Apnea does not reverse intermittent hypoxia-induced bacterial dysbiosis and low-grade endotoxemia in mice. *Sleep* 2016;39(10):1891–7.
- [34] Li J, Zhao F, Wang Y, Chen J, Tao J, Tian G, et al. Gut microbiota dysbiosis contributes to the development of hypertension. *Microbiome* 2017;5(1):14.
- [35] Yang T, Santisteban MM, Rodriguez V, Li E, Ahmari N, Carvajal JM, et al. Gut dysbiosis is linked to hypertension. *Hypertension (Dallas, Tex : 1979)* 2015;65(6):1331–40.
- [36] Hoban AE, Moloney RD, Golubeva AV, McVey Neufeld KA, O'Sullivan O, Patterson E, et al. Behavioural and neurochemical consequences of chronic gut microbiota depletion during adulthood in the rat. *Neuroscience* 2016;339:463–77.
- [37] Desbonnet L, Clarke G, Traplin A, O'Sullivan O, Crispie F, Moloney RD, et al. Gut microbiota depletion from early adolescence in mice: implications for brain and behaviour. *Brain Behav Immun* 2015;48:165–73.
- [38] Haouzi P, Bell HJ, Notet V, Bihain B. Comparison of the metabolic and ventilatory response to hypoxia and H2S in unsexed mice and rats. *Respir Physiol Neurobiol* 2009;167(3):316–22.
- [39] Bavis RW, van Heerden ES, Brackett DG, Harmeling LH, Johnson SM, Blegen HJ, et al. Postnatal development of eupneic ventilation and metabolism in rats chronically exposed to moderate hyperoxia. *Respir Physiol Neurobiol* 2014;198:1–12.
- [40] Burns DP, Roy A, Lucking EF, McDonald FB, Gray S, Wilson RJ, et al. Sensorimotor control of breathing in the mdx mouse model of Duchenne muscular dystrophy. *J Physiol* 2017;595(21):6653–72.
- [41] Burns DP, Canavan L, Rowland J, O'Flaherty R, Brannock M, Drummond SE, et al. Recovery of respiratory function in mdx mice co-treated with neutralizing interleukin-6 receptor antibodies and uroctin-2. *J Physiol* 2018;596(21):5175–97.
- [42] Edge D, Bradford A, O'Halloran KD. Chronic intermittent hypoxia increases apnoea index in sleeping rats. *Adv Exp Med Biol* 2012;758:359–63.
- [43] Dutta A, Deshpande SB. Cardio-respiratory reflexes evoked by phenylbiguanide in rats involve vagal afferents which are not sensitive to capsaicin. *Acta Physiol (Oxford)* 2010;200(1):87–95.
- [44] Lucking EF, Murphy KH, Burns DP, Jaisimha AV, Barry-Murphy KJ, Dhaliwal P, et al. No evidence in support of a prodromal respiratory control signature in the TgF344-AD rat model of Alzheimer's disease. *Respir Physiol Neurobiol* 2018. <https://doi.org/10.1016/j.resp.2018.06.014> S1569-9048(18)30104-6, [Epub ahead of print].
- [45] Turner JR, Rill BK, Carlson SL, Carnes D, Kerner R, Mrsny RJ, et al. Physiological regulation of epithelial tight junctions is associated with myosin light-chain phosphorylation. *Am J Phys* 1997;273(4 Pt 1):C1378–85.
- [46] Edgar RC. Search and clustering orders of magnitude faster than BLAST. *Bioinformatics (Oxford, England)* 2010;26(19):2460–1.
- [47] Caporaso JG, Kuczynski J, Stombaugh J, Bittinger K, Bushman FD, Costello EK, et al. QIIME allows analysis of high-throughput community sequencing data. *Nat Methods* 2010;7:335–6 United States.
- [48] Chao A. Nonparametric estimation of the number of classes in a population. *Scand J Stat* 1984;265–70.
- [49] Faith DP. Conservation evaluation and phylogenetic diversity. *Biol Conserv* 1992;61(1):1–10.
- [50] Bravo JA, Forsythe P, Chew MV, Escaravage E, Savignac HM, Dinan TG, et al. Ingestion of lactobacillus strain regulates emotional behavior and central GABA receptor expression in a mouse via the vagus nerve. *Proc Natl Acad Sci U S A* 2011;108(38):16050–5.
- [51] Cryan JF, Dinan TG. Mind-altering microorganisms: the impact of the gut microbiota on brain and behaviour. *Nat Rev Neurosci* 2012;13(10):701–12.
- [52] Collins SM, Surette M, Bercik P. The interplay between the intestinal microbiota and the brain. *Nat Rev Microbiol* 2012;10(11):735–42.
- [53] Bercik P, Denou E, Collins J, Jackson W, Lu J, Jury J, et al. The intestinal microbiota affect central levels of brain-derived neurotrophic factor and behavior in mice. *Gastroenterology* 2011;141(2):599–609 (e1–3).
- [54] Luczynski P, McVey Neufeld KA, Oriach CS, Clarke G, Dinan TG, Cryan JF. Growing up in a bubble: using germ-free animals to assess the influence of the gut microbiota on brain and behavior. *Int J Neuropsychopharmacol* 2016;19(8).
- [55] Grasa L, Abecia L, Forcen R, Castro M, de Jalon JA, Latorre E, et al. Antibiotic-induced depletion of murine microbiota induces mild inflammation and changes in toll-like receptor patterns and intestinal motility. *Microb Ecol* 2015;70(3):835–48.
- [56] Wurm P, Spindelboeck W, Krause R, Plank J, Fuchs G, Bashir M, et al. Antibiotic-associated apoptotic Enterocolitis in the absence of a defined pathogen: the role of intestinal microbiota depletion. *Crit Care Med* 2017;45(6) (e600–e6).
- [57] Le Roy T, Llopis M, Lepage P, Bruneau A, Rabot S, Bevilacqua C, et al. Intestinal microbiota determines development of non-alcoholic fatty liver disease in mice. *Gut* 2013;62(12):1787–94.
- [58] Li Q, Wang C, Tang C, He Q, Zhao X, Li N, et al. Successful treatment of severe sepsis and diarrhea after vagotomy utilizing fecal microbiota transplantation: a case report. *Crit Care* 2015;19:37.
- [59] Kelly CR, Khoruts A, Staley C, Sadowsky MJ, Abd M, Alani M, et al. Effect of Fecal microbiota transplantation on recurrence in multiply recurrent *Clostridium difficile* infection: a randomized trial. *Ann Intern Med* 2016;165(9):609–16.
- [60] Halkjaer SI, Christensen AH, Lo BZS, Browne PD, Gunther S, Hansen LH, et al. Faecal microbiota transplantation alters gut microbiota in patients with irritable bowel syndrome: results from a randomised, double-blind placebo-controlled study. *Gut* 2018;67(12):2107–15.
- [61] Manichanh C, Reeder J, Gibert P, Varela E, Llopis M, Antolin M, et al. Reshaping the gut microbiome with bacterial transplantation and antibiotic intake. *Genome Res* 2010;20(10):1411–9.
- [62] Kootte RS, Levin E, Salojarvi J, Smits LP, Hartstra AV, Udayappan SD, et al. Improvement of insulin sensitivity after lean donor feces in metabolic syndrome is driven by baseline intestinal microbiota composition. *Cell Metab* 2017;26(4):611–9 e6.

- [63] Jiang ZD, Alexander A, Ke S, Valilis EM, Hu S, Li B, et al. Stability and efficacy of frozen and lyophilized fecal microbiota transplant (FMT) product in a mouse model of *Clostridium difficile* infection (CDI). *Anaerobe* 2017;48:110–4.
- [64] Doi A, Ramirez JM. State-dependent interactions between excitatory neuromodulators in the neuronal control of breathing. *J Neurosci* 2010;30(24):8251–62.
- [65] Teppema LJ, Baby S. Anesthetics and control of breathing. *Respir Physiol Neurobiol* 2011;177(2):80–92.
- [66] Tenorio-Lopes L, Henry MS, Marques D, Tremblay ME, Drolet G, Bretzner F, et al. Neonatal maternal separation opposes the facilitatory effect of castration on the respiratory response to hypercapnia of the adult male rat: evidence for the involvement of the medial amygdala. *J Neuroendocrinol* 2017;29:e12550.
- [67] Sugita T, Kanamaru M, Iizuka M, Sato K, Tsukada S, Kawamura M, et al. Breathing is affected by dopamine D2-like receptors in the basolateral amygdala. *Respir Physiol Neurobiol* 2015;209:23–7.
- [68] Patel S, Majmudar SH. *Physiology, Carbon Dioxide Absorption And Retention*; 2018.
- [69] Brinkman JE, *Physiology Sharma S. Respiratory Drive*; 2018.
- [70] Karbach SH, Schonfelder T, Brandao I, Wilms E, Hormann N, Jackel S, et al. Gut microbiota promote angiotensin II-induced arterial hypertension and vascular dysfunction. *J Am Heart Assoc* 2016;5(9).
- [71] Forsythe P, Bienenstock J, Kunze WA. Vagal pathways for microbiome-brain-gut axis communication. *Adv Exp Med Biol* 2014;817:115–33.
- [72] Lal S, Kirkup AJ, Brunsten AM, Thompson DG, Grundy D. Vagal afferent responses to fatty acids of different chain length in the rat. *Am J Physiol Gastrointest Liver Physiol* 2001;281(4):G907–15.
- [73] Foster JA, Rinaman L, Cryan JF. Stress & the gut-brain axis: regulation by the microbiome. *Neurobiol Stress* 2017;7:124–36.
- [74] Chen JP, van Praag HM, Gardner EL. Activation of 5-HT₃ receptor by 1-phenylbiguanide increases dopamine release in the rat nucleus accumbens. *Brain Res* 1991;543(2):354–7.
- [75] Hosford PS, Mifflin SW, Ramage AG. 5-hydroxytryptamine-mediated neurotransmission modulates spontaneous and vagal-evoked glutamate release in the nucleus of the solitary tract effect of uptake blockade. *J Pharmacol Exp Ther* 2014;349(2):288–96.
- [76] Oliveira LM, Moreira TS, Kuo FS, Mulkey DK, Takakura AC. α 1- and α 2-adrenergic receptors in the retrotrapezoid nucleus differentially regulate breathing in anesthetized adult rats. *J Neurophysiol* 2016;116(3):1036–48.
- [77] Doi A, Ramirez JM. Neuromodulation and the orchestration of the respiratory rhythm. *Respir Physiol Neurobiol* 2008;164(1–2):96–104.
- [78] Richerson GB. Serotonergic neurons as carbon dioxide sensors that maintain pH homeostasis. *Nat Rev Neurosci* 2004;5(6):449–61.
- [79] Fenik P, Veasey SC. Pharmacological characterization of serotonergic receptor activity in the hypoglossal nucleus. *Am J Respir Crit Care Med* 2003;167(4):563–9.
- [80] de Souza Moreno V, Bicego KC, Szawka RE, Anselmo-Franci JA, Gargaglioli LH. Serotonergic mechanisms on breathing modulation in the rat locus coeruleus. *Pflugers Arch* 2010;459(3):357–68.
- [81] Hodges MR, Tattersall GJ, Harris MB, McEvoy SD, Richerson DN, Deneris ES, et al. Defects in breathing and thermoregulation in mice with near-complete absence of central serotonin neurons. *J Neurosci* 2008;28(10):2495–505.
- [82] Hodges MR, Richerson GB. Interaction between defects in ventilatory and thermoregulatory control in mice lacking 5-HT neurons. *Respir Physiol Neurobiol* 2008;164(3):350–7.
- [83] Li A, Nattie E. Serotonin transporter knockout mice have a reduced ventilatory response to hypercapnia (predominantly in males) but not to hypoxia. *J Physiol* 2008;586(9):2321–9.
- [84] Dias MB, Nucci TB, Margatho LO, Antunes-Rodrigues J, Gargaglioli LH, Branco LG. Raphe magnus nucleus is involved in ventilatory but not hypothalamic response to CO₂. *J Appl Physiol (Bethesda, Md : 1985)* 2007;103(5):1780–8.
- [85] Buchanan GF, Smith HR, MacAskill A, Richerson GB. 5-HT_{2A} receptor activation is necessary for CO₂-induced arousal. *J Neurophysiol* 2015;114(1):233–43.
- [86] Messier ML, Li A, Nattie EE. Inhibition of medullary raphe serotonergic neurons has age-dependent effects on the CO₂ response in newborn piglets. *J Appl Physiol* 2004;96(5):1909–19 (Bethesda, Md : 1985).
- [87] Clarke G, Grenham S, Scully P, Fitzgerald P, Moloney RD, Shanahan F, et al. The microbiome-gut-brain axis during early life regulates the hippocampal serotonergic system in a sex-dependent manner. *Mol Psychiatry* 2013;18(6):666–73.
- [88] Lalley PM. D1/D2-dopamine receptor agonist dihydroxidine stimulates inspiratory motor output and depresses medullary expiratory neurons. *Am J Phys Regul Integr Comp Phys* 2009;296(6):R1829–36.
- [89] Nsegebe E, Wallen-Mackenzie A, Dauger S, Roux JC, Shvarev Y, Lagercrantz H, et al. Congenital hypoventilation and impaired hypoxic response in Nurr1 mutant mice. *J Physiol* 2004;556(Pt 1):43–59.
- [90] Vincent SG, Waddell AE, Caron MG, Walker JK, Fisher JT. A murine model of hyperdopaminergic state displays altered respiratory control. *FASEB J* 2007;21(7):1463–71.
- [91] Tuppy M, Barna BF, Alves-Dos-Santos L, Britto LR, Chiavegatto S, Moreira TS, et al. Respiratory deficits in a rat model of Parkinson's disease. *Neuroscience* 2015;297:194–204.
- [92] Oliveira LM, Tuppy M, Moreira TS, Takakura AC. Role of the locus coeruleus catecholaminergic neurons in the chemosensory control of breathing in a Parkinson's disease model. *Exp Neurol* 2017;293:172–80.
- [93] Guyenet PG, Bayliss DA. Neural control of breathing and CO₂ homeostasis. *Neuron* 2015;87(5):946–61.
- [94] Kline DD, Takacs KN, Ficker E, Kunze DL. Dopamine modulates synaptic transmission in the nucleus of the solitary tract. *J Neurophysiol* 2002;88(5):2736–44.
- [95] Beaulieu JM, Gainetdinov RR. The physiology, signaling, and pharmacology of dopamine receptors. *Pharmacol Rev* 2011;63(1):182–217.
- [96] Fujii M, Umezawa K, Arata A. Dopaminergic modulation on respiratory rhythm in rat brainstem-spinal cord preparation. *Neurosci Res* 2004;50(3):355–9.
- [97] Lalley PM. Dopamine1 receptor agonists reverse opioid respiratory network depression, increase CO₂ reactivity. *Respir Physiol Neurobiol* 2004;139(3):247–62.
- [98] Lalley PM. Opioidergic and dopaminergic modulation of respiration. *Respir Physiol Neurobiol* 2008;164(1–2):160–7.
- [99] Fujii M, Umezawa K, Arata A. Dopamine desynchronizes the pace-making neuronal activity of rat respiratory rhythm generation. *Eur J Neurosci* 2006;23(4):1015–27.
- [100] Blesa J, Trigo-Damas I, Dileone M, Del Rey NL, Hernandez LF, Obeso JA. Compensatory mechanisms in Parkinson's disease: circuits adaptations and role in disease modification. *Exp Neurol* 2017;298(Pt B):148–61.
- [101] Gareau MG, Jury J, MacQueen G, Sherman PM, Perdue MH. Probiotic treatment of rat pups normalises corticosterone release and ameliorates colonic dysfunction induced by maternal separation. *Gut* 2007;56(11):1522–8.
- [102] Tulstrup MV, Christensen EG, Carvalho V, Linnings C, Ahrne S, Hojberg O, et al. Antibiotic treatment affects intestinal permeability and gut microbial composition in Wistar rats dependent on antibiotic class. *PLoS One* 2015;10(12):e0144854.
- [103] Wlodarska M, Willing B, Keeney KM, Menendez A, Bergstrom KS, Gill N, et al. Antibiotic treatment alters the colonic mucus layer and predisposes the host to exacerbated *Citrobacter rodentium*-induced colitis. *Infect Immun* 2011;79(4):1536–45.
- [104] Araujo JR, Tomas J, Brenner C, Sansonetti PJ. Impact of high-fat diet on the intestinal microbiota and small intestinal physiology before and after the onset of obesity. *Biochimie* 2017;141:97–106.
- [105] Guo G, Jia KR, Shi Y, Liu XF, Liu KY, Qi W, et al. Psychological stress enhances the colonization of the stomach by *helicobacter pylori* in the BALB/c mouse. *Stress (Amsterdam, Netherlands)* 2009;12(6):478–85.
- [106] Flahou B, Haesebrouck F, Smet A, Yonezawa H, Osaki T, Kamiya S. Gastric and enterohepatic non-*helicobacter pylori* *helicobacters*. *Helicobacter* 2013;18 Suppl 1:66–72.
- [107] El Aidy S, Derrien M, Aardema R, Hooiveld G, Richards SE, Dane A, et al. Transient inflammatory-like state and microbial dysbiosis are pivotal in establishment of mucosal homeostasis during colonisation of germ-free mice. *Benefic Microbes* 2014;5(1):67–77.
- [108] Rooks MG, Veiga P, Wardwell-Scott LH, Tickle T, Segata N, Michaud M, et al. Gut microbiome composition and function in experimental colitis during active disease and treatment-induced remission. *ISME J* 2014;8(7):1403–17.
- [109] Conley MN, Wong CP, Duyck KM, Hord N, Ho E, Sharpton TJ. Aging and serum MCP-1 are associated with gut microbiome composition in a murine model. *PeerJ* 2016;4:e1854.